

# 3-D structure and reflectance measurements

- A system analysis of Lidar Optech ILRIS-3D

HÅKAN LARSSON, TOMAS CHEVALIER, FRANK GUSTAFSSON



FOI, Swedish Defence Research Agency, is a mainly assignment-funded agency under the Ministry of Defence. The core activities are research, method and technology development, as well as studies conducted in the interests of Swedish defence and the safety and security of society. The organisation employs approximately 1000 personnel of whom about 800 are scientists. This makes FOI Sweden's largest research institute. FOI gives its customers access to leading-edge expertise in a large number of fields such as security policy studies, defence and security related analyses, the assessment of various types of threat, systems for control and management of crises, protection against and management of hazardous substances, IT security and the potential offered by new sensors.

Håkan Larsson, Tomas Chevalier, Frank Gustafsson

## 3-D structure and reflectance measurements

- A system analysis of Lidar Optech ILRIS-3d

<b>Issuing organization</b> FOI – Swedish Defence Research Agency Sensor Systems P.O. Box 1165 SE-581 11 Linköping	<b>Report number, ISRN</b> FOI-R--2116--SE	<b>Report type</b> Technical report
	<b>Research area code</b> 4. C4ISTAR	
	<b>Month year</b> September 2007	<b>Project no.</b> E3080
	<b>Sub area code</b> 42 Above water Surveillance, Target acquisition and Reconnaissance	
	<b>Sub area code 2</b>	
<b>Author/s (editor/s)</b> Håkan Larsson Tomas Chevalier Frank Gustafsson	<b>Project manager</b>	
	<b>Approved by</b>	
	<b>Sponsoring agency</b>	
	<b>Scientifically and technically responsible</b>	
<b>Report title</b> 3-D structure and reflectance measurements - A system analysis of Lidar Optech ILRIS-3D -		
<b>Abstract</b> This report describes FOI's scanning laser radar Optech ILRIS-3D. One part is about ILRIS performance, advantages and limits. Another part is about measuring in 3 dimensions and building of 3d-models. We use ILRIS for collecting 3d-information but also for measuring intensity and calculating the reflectance. One chapter describes measurement and calculation of reflectance. The aim with this report is to have a compiled documentation of ILRIS at FOI.		
<b>Keywords</b> Laser radar, Optech ILRIS-3D, Lidar, Performance, 3D, Modelling, Reflectance		
<b>Further bibliographic information</b>	<b>Language</b> English	
<b>ISSN</b> 1650-1942	<b>Pages</b> 55 p.	
<b>Price acc. to pricelist</b>		

<b>Utgivare</b> FOI - Totalförsvarets forskningsinstitut Sensorsystem Box 1165 581 11 Linköping	<b>Rapportnummer, ISRN</b> FOI-R--2116--SE	<b>Klassificering</b> Teknisk rapport
	<b>Forskningsområde</b> 4. Sensorer och signaturanpassning	
	<b>Månad, år</b> September 2007	<b>Projektnummer</b> E3080
	<b>Delområde</b> 42 Sensorer	
	<b>Delområde 2</b>	
<b>Författare/redaktör</b> Håkan Larsson Tomas Chevalier Frank Gustafsson	<b>Projektledare</b>	
	<b>Godkänd av</b>	
	<b>Uppdragsgivare/kundbeteckning</b>	
	<b>Tekniskt och/eller vetenskapligt ansvarig</b>	
<b>Rapportens titel</b> 3-D struktur- och reflektansmätning – En systemanalys av Lidar Optech ILRIS-3D		
<b>Sammanfattning</b> Den här rapporten beskriver den skannande laserradar Optech ILRIS-3D. En del av rapporten utgör en prestandabeskrivning, fördelar och begränsningar. En annan del behandlar 3-dimensionell mätning och byggande av 3d-modeller. Vi använder ILRIS för att samla in 3d-information, men också för att mäta intensitet och beräkna reflektans. Ett kapitel handlar om mätning och beräkning av reflektans. Avsikten med rapporten är att ha ett samlat dokument om ILRIS och dess användning på FOI.		
<b>Nyckelord</b> Laserradar, Optech ILRIS-3D, Lidar, Prestanda, 3D, Modellering, Reflektans		
<b>Övriga bibliografiska uppgifter</b>	<b>Språk</b> Engelska	
<b>ISSN</b> 1650-1942	<b>Antal sidor:</b> 55 s.	
<b>Distribution enligt missiv</b>	<b>Pris:</b> Enligt prislista	

# Contents

1	Introduction .....	7
2	Measurement principle .....	8
3	Performance .....	11
3.1	Laser wavelength and power .....	11
3.2	The beam shape (Pulse width, beam size and divergence) .....	11
3.3	Data sampling rate, spot step, FOV and scanning time .....	12
3.4	Maximum and minimum distance .....	13
3.5	Accuracy .....	14
3.6	Power supply and consumption .....	16
3.7	Environmental.....	17
3.8	Physical data .....	17
4	IO interfaces .....	18
4.1	Analogue outputs .....	18
4.2	Ethernet connector .....	18
4.3	USB connectors .....	18
4.4	Serial connector .....	19
4.5	Antenna for WiFi .....	19
5	Operator interface.....	20
5.1	Controller .....	20
5.2	Parser.....	21
6	The influence on measurements by external factors .....	22
7	3-D measurements and modeling. ....	29
7.1	PIFEdit and PolyWorks .....	30
7.2	Texturing models .....	37
8	Reflectance information from intensity data .....	43
8.1	Reflectance target.....	43
8.2	ILRIS presentation of intensity over the distance.....	45
8.3	Method for reflectance calculations .....	46
8.4	Error analysis of calculated reflectance .....	48
8.5	Calculation of laser cross section of a target .....	50
9	Measurements from the analogue outputs.....	51
10	References .....	52

APPENDIX A Address to Optech and useful contact information

APPENDIX B Spatial resolution [m] at various distances for different spot spaces (SS)

APPENDIX C Acquisition time for different spot steps for fractions of full FOV



# 1 Introduction

In 2001, FOI Laser systems acquired an Optech ILRIS-3D (henceforth called ILRIS) scanning 3-D laser radar. The unit was exchanged in September 2005 to an improved version. The reason for replacement was that the old unit was of a very early edition built in obsolete technology (the third unit ever built<sup>1</sup> and the first unit for the open market). With the new unit, we have a very modern laser radar system with better performance and we have the possibility to provide ILRIS with other features such as external camera, GPS etc.

This report describes the laser radar system ILRIS, its performance, applications and data evaluation methods. In chapter 2 the measurement principle is discussed. In chapter 3 the performance is presented. Chapter 4 is about the in- and outputs and chapter 5 about the operators user interface. Chapter 6 describes the influence on measurements by external factors. Chapter 7 is about 3-D measurements and modeling. The modules in the PolyWorks software are described shortly. In chapter 8 reflectance measurements and the evaluation methods for calculating reflection are discussed. Chapter 9 describes how measurements are made with analogue outputs. The aim with this report is to have a compiled documentation of ILRIS.

ILRIS is a scanning laser radar equipment and acquires 3-dimensional point clouds. It contains a laser, a detector and an advanced mechanical deflection of the laser beam. Figure 1 shows the front side and back side of ILRIS. On the front is a shaded window which the laser beams pass through and the internal digital video camera is located in the upper right corner. On the back is the operator window (17-cm LCD VGA viewfinder (640 x 480 pixel), with text panel for status messages) where an image from the digital video camera is shown and to the right are the interfacing connectors.

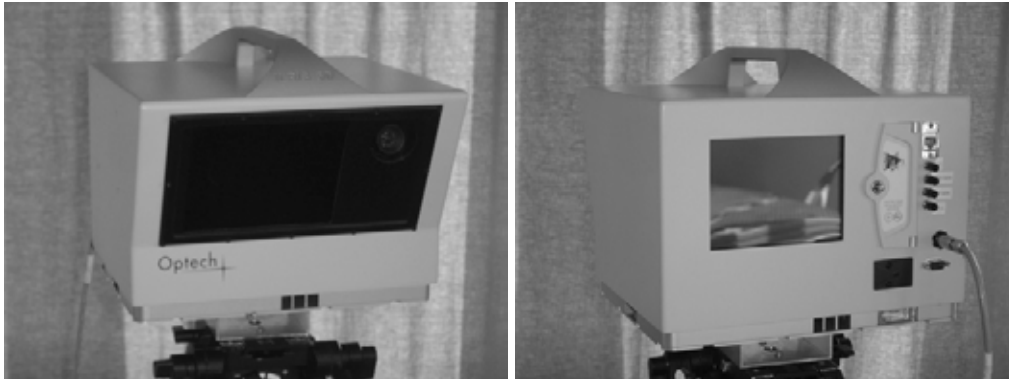


**Figure 1. The laser scanner ILRIS-3D, front view to the left and back view to the right.**

ILRIS is manufactured by Optech Incorporated<sup>1</sup>. The company is based in Toronto, Ontario, Canada. Appendix A contains address to Optech and useful contact information.

---

<sup>1</sup> The first unit of Optech ILRIS-3D was built already 1993 (!), but Optech didn't see any potential for further developing at that time.



## 2 Measurement principle

ILRIS is based on the laser radar technology, also called Lidar (light detection and ranging). In principle, it works like ordinary radar, except that the system sends out laser pulses rather than radio waves. The reflected light is collected with the receiver. Knowing the time it takes for a light pulse to travel to an object and back to the receiver, we can calculate the distance to an object as:

$$\text{Distance} = (\text{Speed of light} \times \text{Time of flight})/2 \quad (1)$$

An illustration of the principle of time-of-flight (TOF) is shown in Figure 2. The start pulse is sent from the laser and starts a counter, counting cycles of a known frequency. When return pulse hits the detector the counting stops.

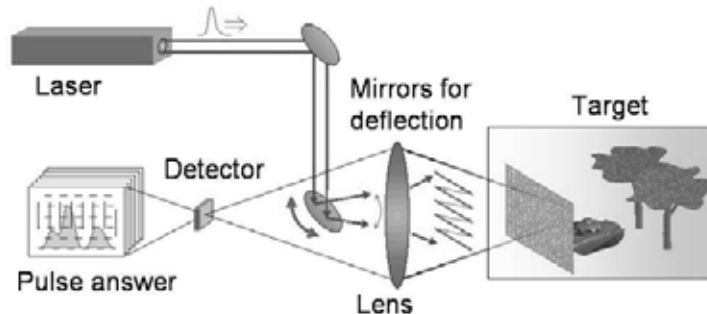


**Figure 2. The principle of a scanning laser radar system using the Time of Flight technology. A laser generates an optical pulse and mirrors take care of the deflection (between two laser shots). The laser pulse is reflected by an object and returns to the receiver. A high-speed counter measures the time of flight from the start pulse to the return pulse. The time measurement is converted to a distance by using the formula above (1).**

The laser beam is deflected in the vertical and horizontal direction between every laser shot by two mirrors mounted on galvanometers, one for vertical and one for horizontal. The distance and deflection for every single laser shot (x-, y and z-coordinate) will be calculated for each point and all points can be presented together as a point cloud. Figure 3 shows a typical point cloud containing hundred thousands of points. If the point cloud is viewed from the same direction as the recording is made, the image will look 2-dimensional. Rotating the point cloud will make the image look 3-dimensional and also revealing shadows in the image.



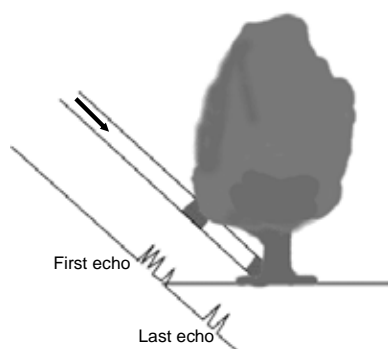
**Figure 3. To the left a point cloud viewed in the same direction as the recording was made (the image will look 2-D). To the right the same point cloud rotated from the recording direction.**

The amplitude of the returning signal is the intensity of the point. ILRIS works with two gain domains, high and low. The high gain goes from 0 to 255 digits and low gain goes from 300 up to 25500 digits (totally 9 bits). It is a factor 100 between the domains.

Optech's data processing software can categorize detected laser pulses according to the reflectance of the target surface. The output is presented as a grey scale in 256 units (converted from 9 to 8 bits). In Figure 3 we see the intensity data as a greyscale in 256 steps (0 for black to 255 for white).

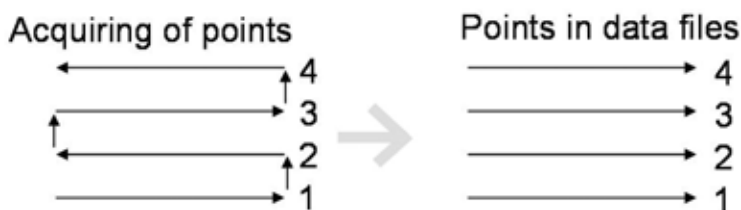
ILRIS works with two detection modes, first or last echo. This means that a laser pulse that is partly transmitted through some sparse material (such as vegetation, camouflage net, etc.) and reflected from a target surface behind the concealment can be detected by the sensor in the last echo mode. In other words, the laser pulse must have a free line of sight for detection, at least, a part of the beam's cross section and the energy of the return must exceed the detection threshold. We refer to this as "penetration".

Figure 4 shows an illustration of first or last echo mode. First echo measures the range to the first object encountered - in this illustration, the tree foliage. Last echo measures the range to the last object - in this case, the ground.



**Figure 4. First or last echo can be selected on the ILRIS-3D. First echo – the tree foliage, last echo – the ground.**

ILRIS works with a step and stare sweep, and always starts the scan in the lower left corner. The first sweep goes from left to right. After that, the vertical mirror steps once and a new sweep starts, this time from right to left. All sweeps from right to left will have their points presented in opposite direction in the data files.



**Figure 5. To the left shows how the acquiring of data is made in sweeps from left to right, step, right to left, step and so on. The presentation of points per row in files is always made from left to right.**

ILRIS internal coordinate system is oriented as shown in Figure 6. X is the horizontal position, Y is the distance and Z is the vertical position.

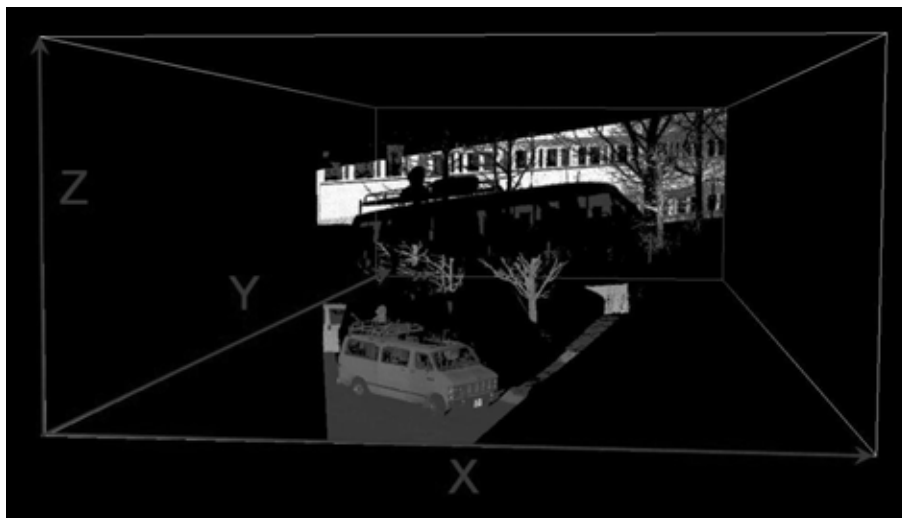


**Figure 6. The orientation of ILRIS internal coordinate system. X is the horizontal position, Y is the distance and Z is the vertical position.**

### 3 Performance

Technical data for ILRIS are shown in Table 1 and are discussed in the following chapters (3.1 to 3.5).

**Table 1. Technical data for Optech ILRIS-3D**

<b>Performance</b>		
Wavelength	1.541 $\mu\text{m}$ (NIR)	(Chapter 3.1)
Laser power	10 mW	(Chapter 3.1)
Laser class (IEC 60825-1)	Class 1 for the scanning beam	(Chapter 3.1)
Pulse width	~5 ns	(Chapter 3.2)
Beam size	12 mm (outgoing)	(Chapter 3.2)
Beam divergence	170 $\mu\text{rad}$ (0.00974°)	(Chapter 3.2)
Data sampling rate (actual measurement rate)	2000 points per second	(Chapter 3.3)
Minimum spot step	26,6 $\mu\text{rad}$ (0.0015°)	(Chapter 3.3)
Scanner field of view	40°x40° ( $\pm 20^\circ$ )	(Chapter 3.3)
Maximum distance	350 m (4 % reflectance) 800 m (20 % reflectance)	(Chapter 3.4)
Minimum distance	3.2 m	(Chapter 3.4)
Raw range accuracy	7 mm @ 100 m (Sigma 1)	(Chapter 3.5)
Raw positional accuracy	8 mm @ 100 m (Sigma 1)	(Chapter 3.5)

#### 3.1 Laser wavelength and power

The laser wavelength is 1.541  $\mu\text{m}$  and the pulse repetition frequency (PRF) is 2000 Hz. The power is 10 mW (out from ILRIS after the shaded window) which is the power limit at 1.5  $\mu\text{m}$  for an eye-safe class 1 laser. Observe, the measurements head is not allowed to be open under any circumstances. The laser power directly after the laser is higher and not eye-safe.

#### 3.2 The beam shape (Pulse width, beam size and divergence)

The pulse width is approximately 5 ns. It varies from laser to laser.

ILRIS output beam divergence (full angle) measured at  $1/e^2$  of intensity is less than 200 $\mu\text{rad}$  (170  $\mu\text{rad}$  typical; equal to 0.00974°). Waist is 6mm (12mm diameter) typical. Ideally, the waist location should be at the collimator (beam expander) exit, i.e. ~0.2m inside of the device. Practically, considering optical adjustment accuracy, it can be within +/-40m range. That can slightly affect the spot size at short ranges (up to 100m) but does not change the long-range pattern. The spot diameter at  $1/e^2$  level is calculated as

$$d = \sqrt{0,012^2 + (0,00017r)^2} \text{ [m]} \quad (2)$$

where d is the diameter in m, r is the distance.

The beam shape has a Gaussian distribution based on  $1/e^2$ .

### 3.3 Data sampling rate, spot step, FOV and scanning time

The data sampling rate (actual measurement rate) is 2000 points per second. A normal scan containing thousands of points takes several minutes to acquire.

A spot step is the angular increment between two scan points and can be adjusted. ILRIS works with totally 100 spot steps, each based on a multiple of  $26.67 \mu\text{rad}$ . Spot step 1 is the interval between two points where the mirrors move  $26.67 \mu\text{rad}$ , spot step 2 is  $53.3 \mu\text{rad}$  and so on.  $26.67 \mu\text{rad}$  is equal to 2.67 mm resolution both vertical and horizontal at a distance of 100 m. The spatial resolution is programmable; the operator can choose the resolution of a target at a certain distance. Figure 7 shows the resolution as function of distance for different spot steps (SS). Appendix B contains the graph values from Figure 7.

The full field of view (FOV) is  $40^\circ \times 40^\circ$ . The FOV is programmable and is set indirectly by the operator while setting the region of interest (ROI), which is the area where ILRIS will acquire data.

The time for scanning a view depends on the FOV and resolution. Figure 8 and Figure 9 shows time for scanning a view with different resolution (spot step) referring to Figure 7. Different cover grade of FOV are shown in these graphs. Appendix C contains values of time for acquiring a view as function of spot step based on cover grade of full FOV

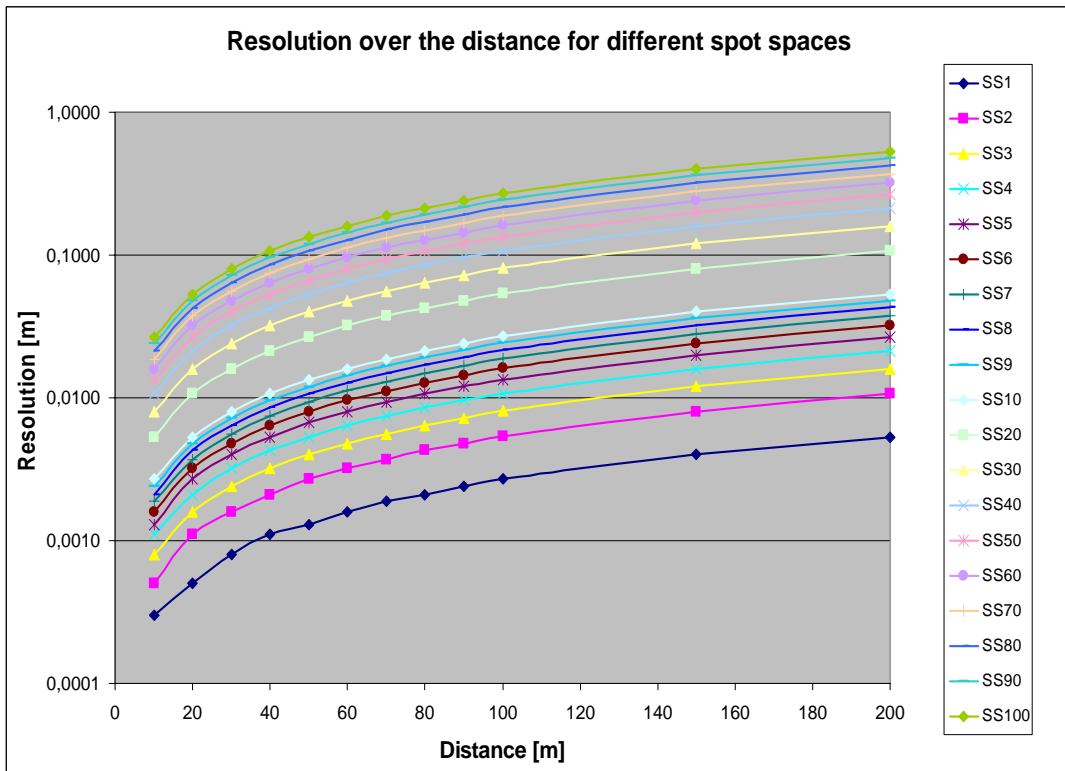


**Figure 7. Resolution [m] versus distance [m] for different spot steps.**

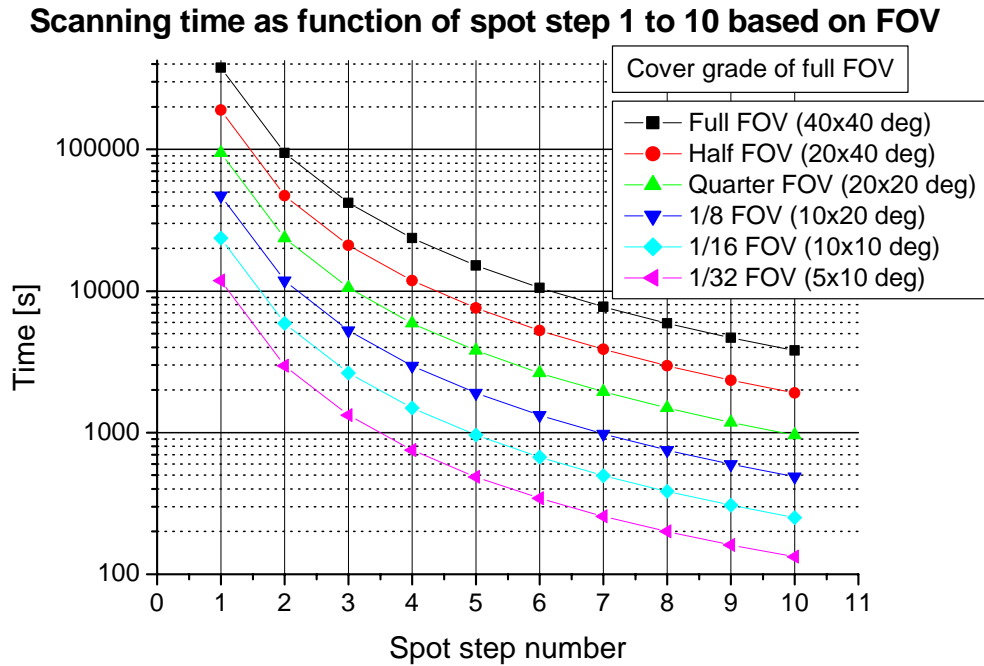


**Figure 8.** Graph shows acquisition times for different resolution and FOV for various spot settings 1 to 10.

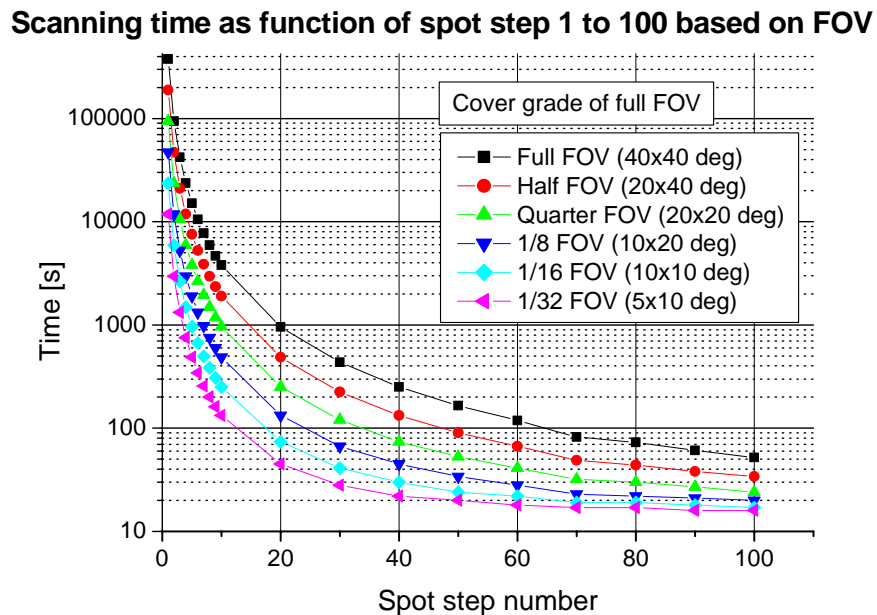


**Figure 9.** Graph shows acquisition times for different resolution and FOV for various spot setting 1 to 100.

### 3.4 Maximum and minimum distance

According to the specification, 4 % reflectance is enough for a return signal over a 350 m distance measurement. That value is based upon a surface at normal incidence. The beam very rarely hits surfaces at such low angle of incidence. The return will be lower with higher angle and that will influence the detection range. The experience is that the return will be sufficient from most objects up to 200 m (objects with very low reflectance and hit with a very oblique angle of incidence excepted).

The minimum distance is about 3.2 m (based on the long pulse width about 10 ns from earlier versions of ILRIS). The laser pulse is entirely out in the air before the detection algorithm allows detection (Figure 10). With a pulse width of 5 ns the minimum distance could be around 1.6 m. Allowing a shorter target distance than the pulse width would lead to a mixed signal of the outgoing pulse (first detected as stray light) and the first hit, resulting in an erroneous distance measurement, a so called artifact (or ghost point).



**Figure 10. The laser pulse is entirely out in the air before the detection algorithm allows detection.**

### 3.5 Accuracy

In the specification Optech states the “raw range accuracy” to be 7 mm (Sigma 1). The quoted accuracy holds or is exceeded through most of this dynamic range and absolutely holds if applied to samples across the complete dynamic range. For very weak returns (approximately the lower 5% of the dynamic range), the accuracy will drift beyond this specification.

We have measured and calculated the standard deviation (Sigma 1) for the range by measuring eight reference surfaces with different reflectance. The standard deviation is calculated from hundreds of points. In Figure 11 you see calculated standard deviation every fifth meter from 10 to 70 m. We can clearly see that the standard deviation drift beyond the specification for weak returns. We can also see three peaks, one for 61.9 % reflectivity, one for 48.8% and one for 29 % and we can also see how the standard deviation has started to increase over the distance for the 98.8 % surface. What we see is a mixture of the two gain domains that ILRIS has. There are points in both high and low gain domains and the two domains present the distance mismatched; this is due to the use of the dynamic range in a very adverse way and to the detection algorithm.

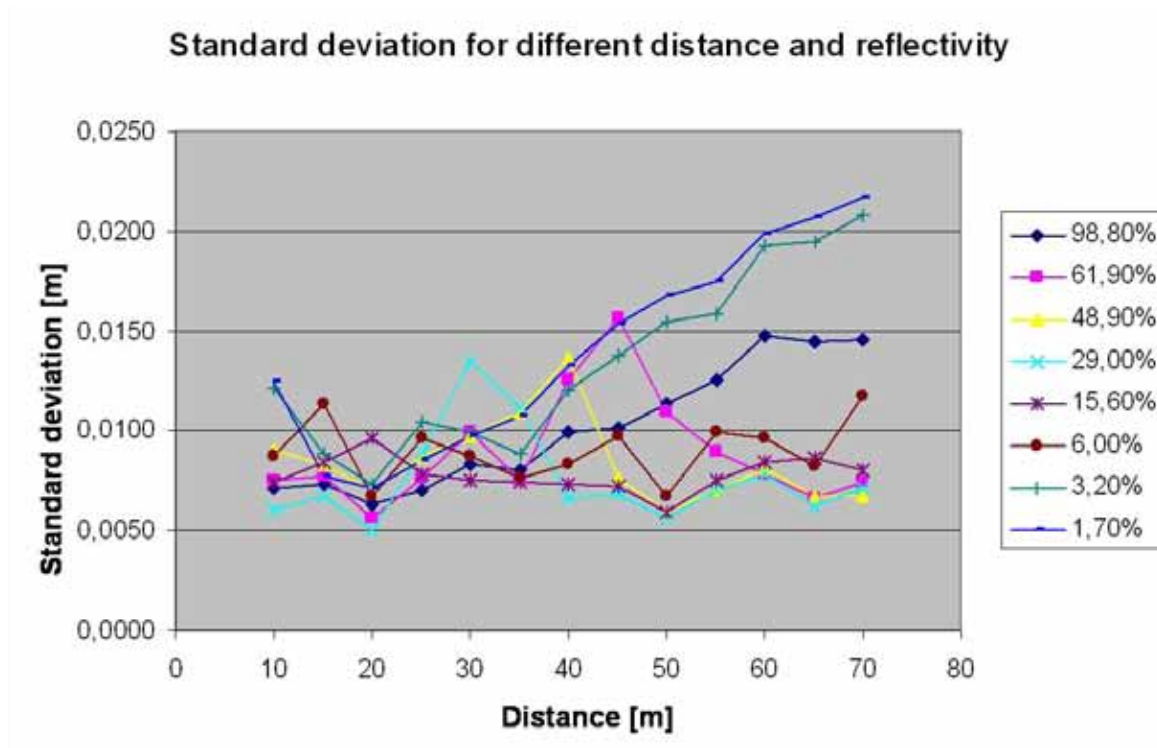


**Figure 11. Standard deviation for various target reflectances.**

The raw positional accuracy is harder to verify, but we can look at it visually. Figure 12 shows an example of an ortographical representation of a surface on a grid. The points are not exactly positioned in rows and columns, showing the position error. We can see that the positions are inside the specified 8 mm (Sigma 1)

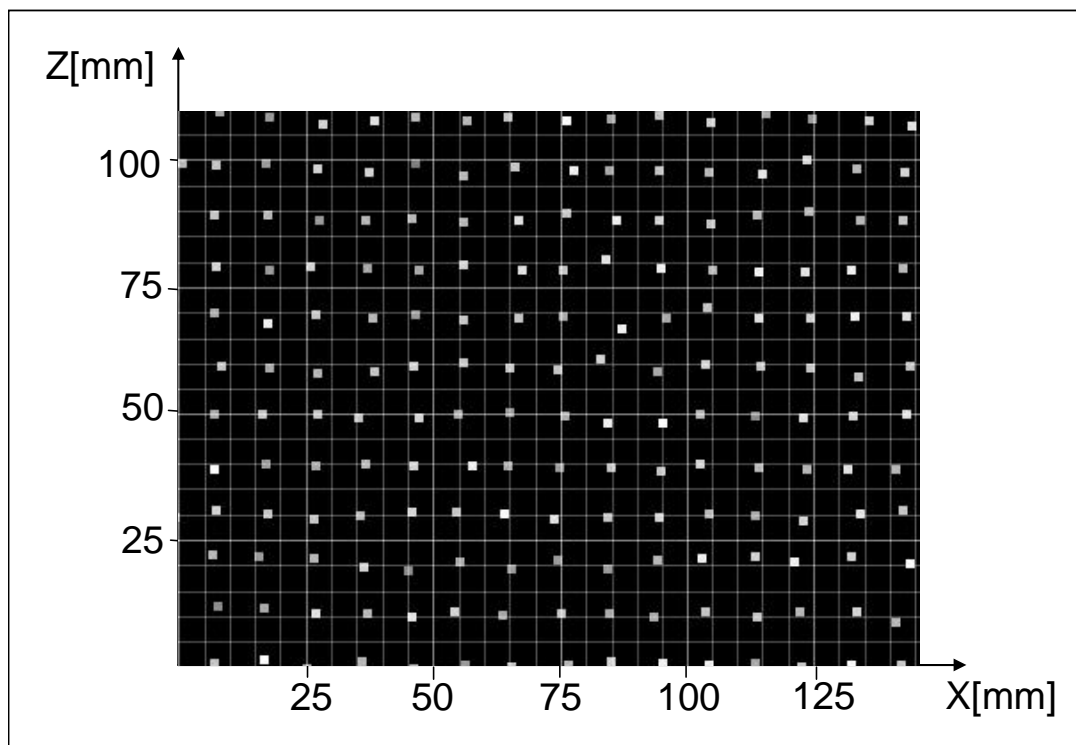


**Figure 12. An ortographical representation of a part of a point cloud presented on a grid. Some deviation of the points from the grid can be seen, but inside the specified tolerance of 8 mm (Sigma 1).**



### 3.6 Power supply and consumption

**Table 2. Power supply and consumption**

---

<b>Power supply and consumption:</b>	
Power supply	24-32 VDC
Consumption	75 W nominally

---

ILRIS power supply is 24-32 VDC and can be run either with battery packages or with external power supply. The power consumption is 75 W (including a turn table that is not included in the FOI system – hence the consumption for our unit is a bit lower). The batteries are of type Anton Bauer<sup>2</sup> Hytron 120 14.4-volt, 100-Whr, and nickel metal hydride battery. The charger is of type 2722 dual battery Power Charger. Normally, a battery charge is enough for 4 hours operation for a battery pair (without turn table). To avoid power interruption a hot-swap is made, which means that charged batteries are mounted in the battery holder (Logic Series Gold Mount) before the recharged are removed.

A voltage in excess of 32 V will lead to burned components and a too low voltage will lead to a shut down. A too low voltage when booting ILRIS will make the hard disc not start properly (an error message saying the operating system cannot be found will appear, which in fact is not the case).



**Figure 13. Pair of batteries placed in a charger to the left and to the right a pair of batteries placed in the holder.**

### 3.7 Environmental

**Table 3. Environmental data of Optech ILRIS-3D**

---

<b>Environmental:</b>	
Operating temperature	0°C to +40°C (with special use of working -20°C)
Storage temperature	-20°C to +50°C
Weather protection	NEMA 4X, water and dust protected

---

According to the specification the operating temperature is 0°C to 40°C. With special measures it is possible to operate down to -20°C. In this case it is very important to power on ILRIS indoors and warms it up about one hour before taking data. The heat inside ILRIS is then enough to hold the temperature over 0°C. Never start ILRIS below 0°C if it is not warmed up before. A temperature inside ILRIS below 0°C will affect the system and the acquisitions will go outside specification regarding accuracy. An inside temperature under -20°C will make the glue to the mirrors crystallize and the mirrors will fall off. Hence, ILRIS should never be stored below -20°C.

Avoid direct sunlight in warm weather. Temperature inside ILRIS in excess of 40°C will lead to a shut down. If this occurs ILRIS can be cooled down for an hour with open memory door.

ILRIS is weather protected against water and dust. The scanner is splash-resistant, but not designed to withstand heavy rain.

### 3.8 Physical data

**Table 4. Physical data of Optech ILRIS-3D**

---

<b>Physical data:</b>	
Physical size (Measurements head) (LxWxH)	320x320x225 mm
Weight	approx. 11,4 kg

---

## 4 IO interfaces

Figure 14 shows all the connectors at the back of ILRIS.



**Figure 14. The connectors at the back of ILRIS. To the upper left is a door covering two USB connectors for memory stick, in the lower left is an antenna for WiFi. Upper right is an Ethernet connector. Below that are four SMA Bulk head connectors for analogue outputs and below that there is a power connector and the lower right is a serial connector.**

### 4.1 Analogue outputs

On the back of ILRIS there are four SMA bulk head connectors for analogue outputs of detector signals (two gain domains; high and low), laser trigger and line trigger. The two gain domains are both 8 bits (0-255), but with a difference of a factor 100. High gain goes from 0 to 255 digits and low gain from 300 up to 25500. These connectors have been provided by Optech in order to monitor the full waveform from the detector. The signals can afterwards be improved with signal processing algorithms. More about the analogue signals can be read in chapter 5.

### 4.2 Ethernet connector

A PC or handheld computer (HP iPAQ) is used for controlling ILRIS. Connection is made via IP-addresses through Ethernet RJ45 interface. Speed is 10/100 Mbit Ethernet.

### 4.3 USB connectors

Storing data to external memory stick is made through two USB connectors which are placed behind the door. Only one memory can be placed in one connector at a time. The ports work as redundancy for each other. The USB memory must be formatted as FAT. When booting ILRIS the memory stick is not allowed to be connected. ILRIS will read from the memory and overwrite ILRIS firmware SCADA. If this happens the SCADA program has to be reinstalled which is made from the memory stick through one of the USB connectors.

#### 4.4 Serial connector

The operative system JRC is installed through the serial connector. A twinned cable must be used with pin 2 and 3 shifted (Modem cable).

#### 4.5 Antenna for WiFi

At the back there is also a black plate, which is the antenna for WiFi (Wireless LAN). WiFi can be used up to 7.6 m between ILRIS and PC or handheld computer.

## 5 Operator interface

PC or handheld computer (HP iPAQ) is used for controlling ILRIS. ILRIS can be operated via wire (Ethernet) or wireless (WiFi).

### 5.1 Controller

The Controller program is developed to operate both on PC or handheld computer (HP iPAQ) and is the operator interface to ILRIS.



**Figure 15. The Controller program interface. The square in the image from the internal video camera shows a ROI set by the operator.**

The Controller program provides a graphical real-time display of ILRIS-3D scan settings and operation. You can use the Controller to:

- Capture images from the ILRIS-3D camera
- Program a scan, defining and adding regions of interest (ROI)
- Start and stop a scan
- Monitor the scanner hardware
- Monitor the progress of a scan.

A complete operating description will not be presented in this report; this can be found in other document<sup>3,4,5</sup>.

## 5.2 Parser

An acquired view will be stored as compressed metafile (data together with a header and a picture in jpg format). The parser processes the data so that is suitable for processing by CAD, GIS or other modeling software. Formats we use are

- PIF    which is used for the PolyWorks<sup>®</sup>. PolyWorks is used for 3d-modelling and visualization. Extension is pf and the file is binary. The intensity has a floating limit between high and low gain for best visualization.
- XYZ    ASCII files with Cartesian x-, y- and z-coordinates and an intensity value. X is horizontal position, y is the distance and z is the height. The intensity has a floating limit between high and low gain for best visualization. As it is an ASCII file this format can be used in any application that can read and visualize ASCII in 3 dimensions.
- RAW    ASCII files with spherical x-, y- and z-coordinate and an intensity value. X and y is horizontal and vertical position from ILRIS internal angle transducers. Z is the distance. We use this format for reflectance calculations described in chapter 8. The intensity from 0 to 127 is represented of high gain and 128 to 255 of low gain.

Other formats that we don't use are PTX, 3DV, BWP, S3D, PTC, BLF, IVA and IXF.

IXF is an industrial standard for laser radars and a format that in future time will be the big 3d format (words from Optech). The format can be found as open source code on Internet.

## 6 The influence on measurements by external factors

This section describes how the measurements are affected by some external factors.

Are measurements affected by...

- **...tripod leveling?**

*Not required.* Rough leveling is sufficient. ILRIS does not have to be set up over known points.

- **...reflectance of the object?**

*Not usually.* Highly reflective objects may saturate the laser detector, while the return signal from low-reflectance objects may occasionally be too weak to register as valid. Figure 16 shows one example of saturated data (aluminium foil) and one example of too weak signals.

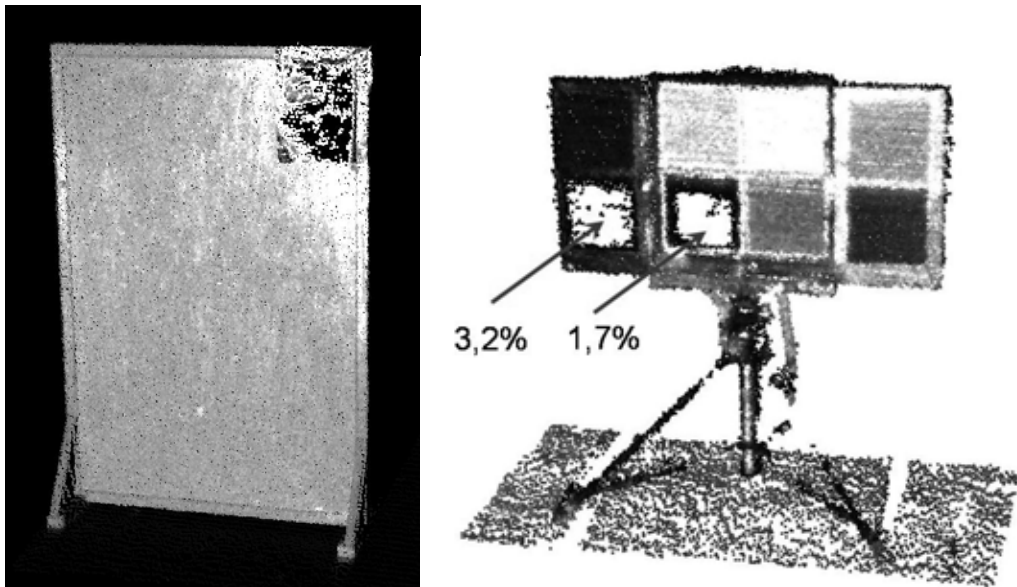


**Figure 16.** Left image shows how a piece of aluminium foil (upper right corner in image) is saturated. Right image shows some reflectance surfaces and in this case the two lowest reflectance surfaces have most points registered invalid because of a too weak signal.

- **...day or night?**

*No.* Laser radar is an "active illumination" technique that, unlike photography, does not depend on ambient illumination. It works during the day or at night.

- **...sunlight and reflections/angle of measurement?**

*Sometimes.* A strong sunlight reflection off a highly reflective target may saturate a receiver, producing an invalid or less accurate reading. However, laser measurements are not usually affected by other reflections. ILRIS laser pulses within a preferred range of angles. ILRIS is designed to operate in daylight. Avoid strong backlight or the sun right in back of the scanner, which might affect the probability of detection.

- **...dust and vapor?**

*Yes.* Laser measurements can be weakened by interacting with dust and vapour particles, which scatter the laser beam and the signal returning from the target. However, using last-pulse measurements can reduce or eliminate this interference. Serious dust as mud will decrease the distance for detection while mud has a rather low reflectance at 1541 nm.

- **...background noise and radiation?**

The laser is not normally affected by background noise. Avoid direct sunlight. While the sun has components of 1541 nm it can affect the measurement.

- **...temperature and temperature variations outdoor?**

*No.* The laser is unaffected by pressure or vacuum variations, or off-gas layers.

- **...inside temperature of ILRIS?**

*Yes.* When measuring the same static scene we have noticed that both the distance and the intensity are affected by the internal temperature of ILRIS. Figure 17 shows that it takes about an hour to get ILRIS steady in distance when measure the same static scene. The 98.8 %, 61.9 %, 29.0 % and 1.7 % reflectance targets was placed about 7 cm longer in distance compared to the other four targets. We can see that the individual distances follow each other but decreases about 3-5 cm each. Normally this doesn't matter as long as the whole scene is affected the same way. When measure a known distance for comparing an earlier distance with a new one there is problems. Optech is aware of the problem, but for the moment they haven't solved it.

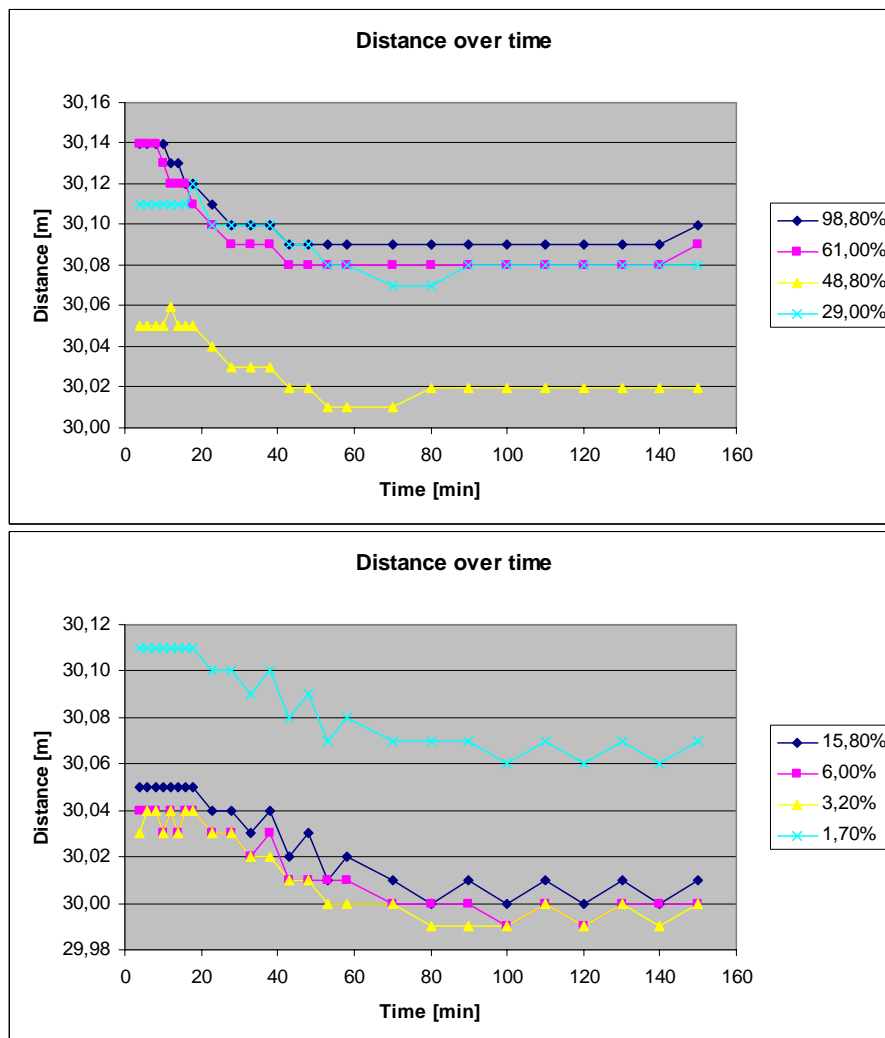


**Figure 17. Static measurement of distance over time. It takes about an hour to get stable.**

Even the intensity is affected by the internal temperature of ILRIS. A measurement of the intensity over time of a static scene shows how the intensity increases over time, see Figure 18. Normally this is no problem as long as we use the intensity for visualization. When using ILRIS as measurement equipment for reflectance measurements we must have a



calibrated reflectance target in view to measure the intensity of known reflectances. More about this in chapter 8.

Intensity over time for different reflectance

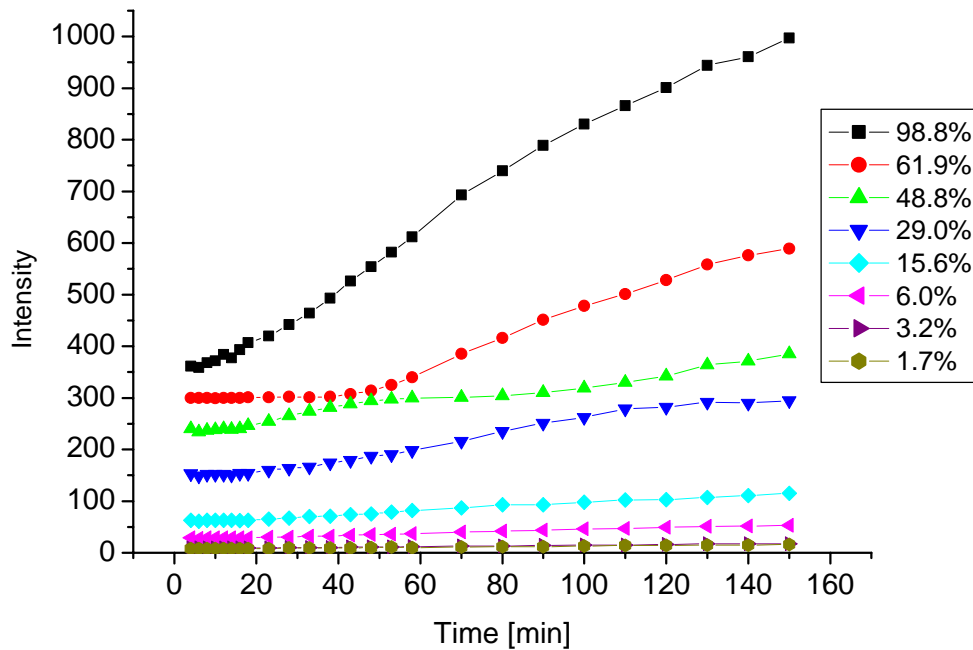
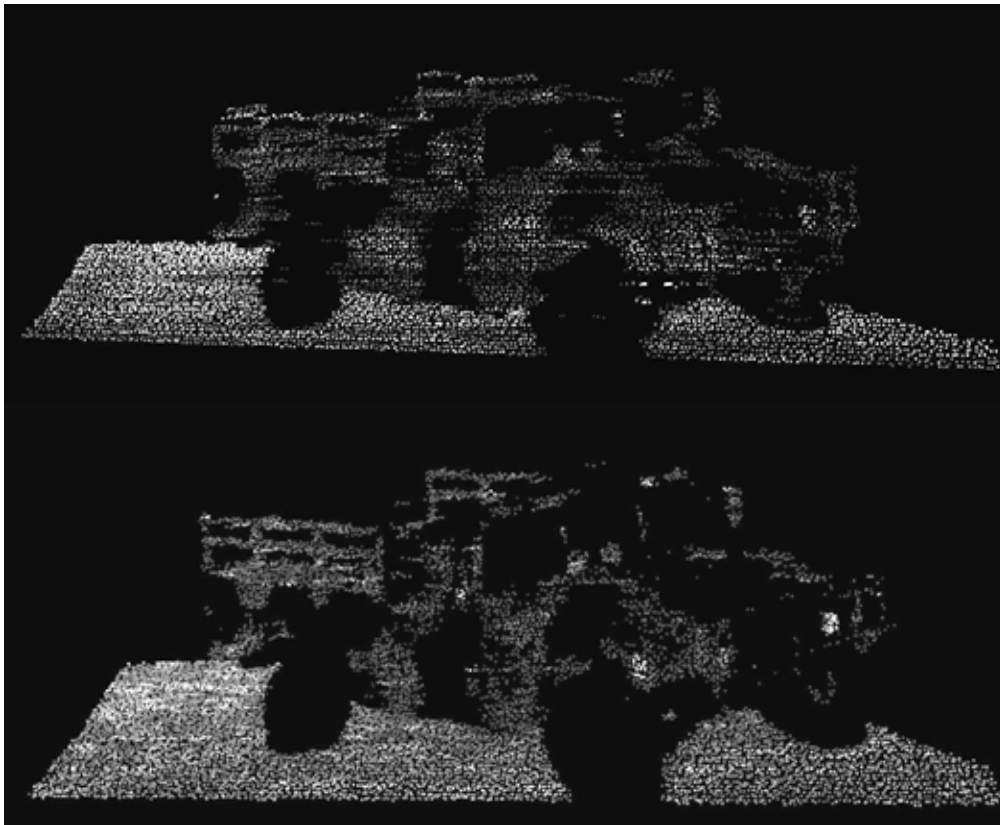


Figure 18. Measured mean intensity at the reflectance surfaces over time.

- ...scintillation?

*Yes.* Scintillation will cause fluctuations in the return signal and hence a decreasing detection distance. The scintillation can be seen in the intensity as well. See Figure 19 for an example. When upper view was acquired there was a temperature difference of 40°C between indoor and outdoor temperature. The scintillation in the air can clearly be seen in the intensity, look especially at the vehicle. Lower image shows the same view with the indoor temperature as cold as possible. Now there is not as much scintillation as before.



**Figure 19. Two measurements acquired of the same scene. In upper view the temperature difference indoors and outdoors is about 40°C and there is a strong scintillation. In the image below the temperature difference has decreased and the scintillation as well.**

- **...target's angle of incidence?**

*Yes.* Laser measurements can be made to targets at any angle. However, the amplitude of the return signal will be weaker and weaker when going towards oblique angles. Hence the signal can be too weak for detection, particularly if the surface has a low reflectance.

- **...the hit of a surface?**

*Yes.* As long as the whole cross section of the illuminating beam hits a surface, the presented distance will be within the specified distance tolerance. There are however problems when the beam hits an edge or passes through a semitransparent material. Figure 20 and Figure 21 show images from a measurement where edge effects were studied. A target containing a rope and a plank were measured with an elevation so the ground was the background in the view. The images show how the intensity values will decrease at the edges. Depending on whether first or last pulse has been detected, the decreased intensity points will be at the rope and plank or at the ground. In Figure 21 we can clearly see artifacts between both the rope and the plank to the ground presented with wrong distances (point cloud seen from the side; scan direction from the left follow the arrow in the image pointing out  $\approx 1.7$  m). Using the last pulse mode results in artifacts even below ground level and in front of the target. No clear difference could be found between a thin target, where the laser cross section is split with sections on both sides of the target (the rope), and a target with just one split of the cross section (the plank). Theoretically such artifacts can occur when the beam hits more than one object, where the distance between the objects is shorter than the pulse length. For our ILRIS it seems to be at a distance about 1.7 m and that is equal to 5.7 ns which should be our laser's pulse length.

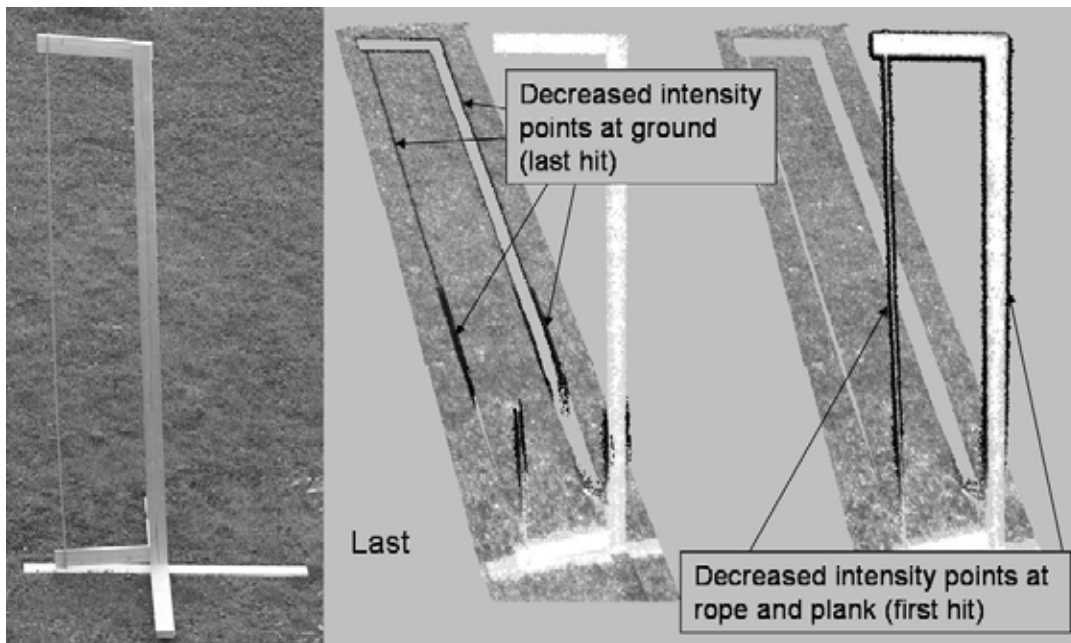


**Figure 20. Images from a measurement checking edge effects. Left image shows the measurement performance**

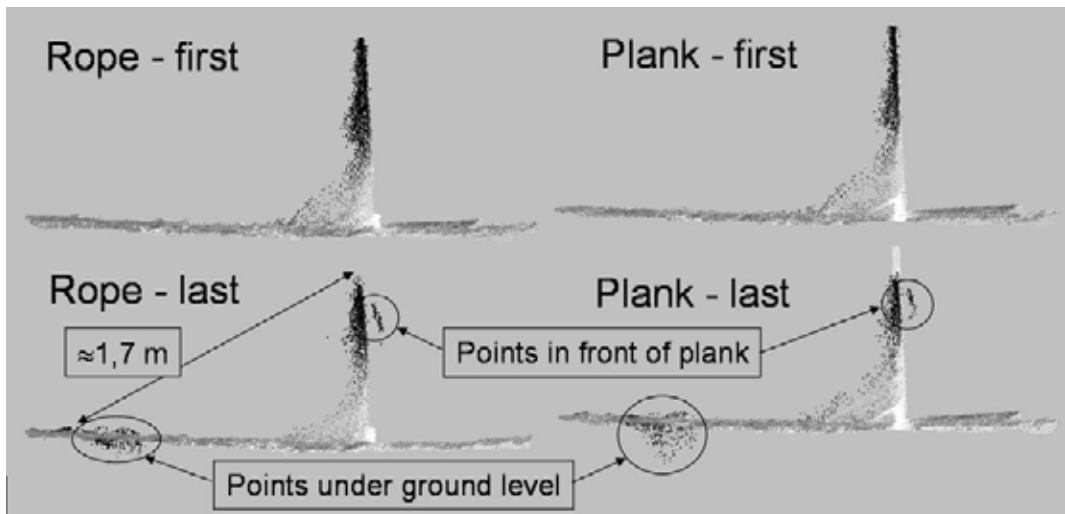


**Figure 21. Images shows artifacts between target and the ground. When using last echo mode artifacts occur even in front of target and under ground level.**

When looking at a penetration of a semitransparent material we see the same phenomena. Figure 22 shows measurement performance of a curtain with a reflectance target in back of the curtain. The curtain is of a semitransparent material. The reflectance target has been moved in steps of 10 cm from 50 cm to 130 cm from the curtain. Only last echo mode has been used. Figure 23 shows a series of images where we can see how the spread of artefacts changes with the distance between curtain and reflectance target. Scan direction is from the right. We can see how the range within which ghost points appear decreases with increasing separation distance between first and second echo. At 50 cm separation the whole region between the physical targets is full of ghost points. At 130 cm separation, that ghost points appear just a few cm from the targets. In Figure 24 we see how the laser beam has passed through the curtain at 200 cm separation distance between curtain and reflectance target (most points at reflectance target), but at 180 cm most points are at the curtain (indicating that the laser pulse length is longer than the target separation distance). We can draw the conclusion that the laser pulse length in this case is somewhere between

180 to 200 cm; equal to 6.0 - 6.7 ns (the curtain acquisitions was made with our old unit of ILRIS and therefore a bit longer pulse compared to the “rope-plank” measurement). We can see a square of points at the curtain and those points actually correspond to the 1.7 % reflectance target. The signal from this reflectance target is too low to be detected and therefore the last pulse over the threshold will be at the curtain.

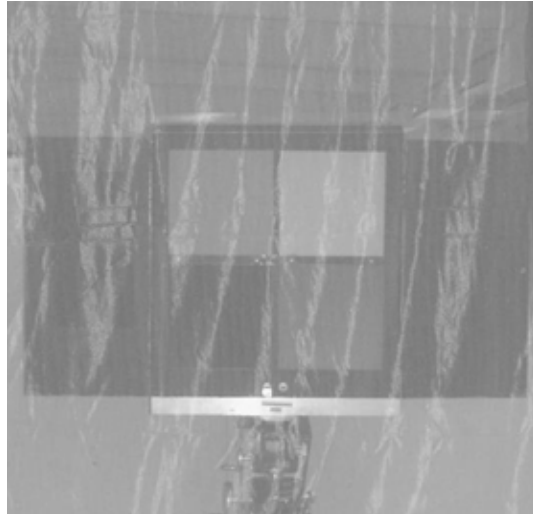


**Figure 22. Curtain with a reflectance target behind the curtain**

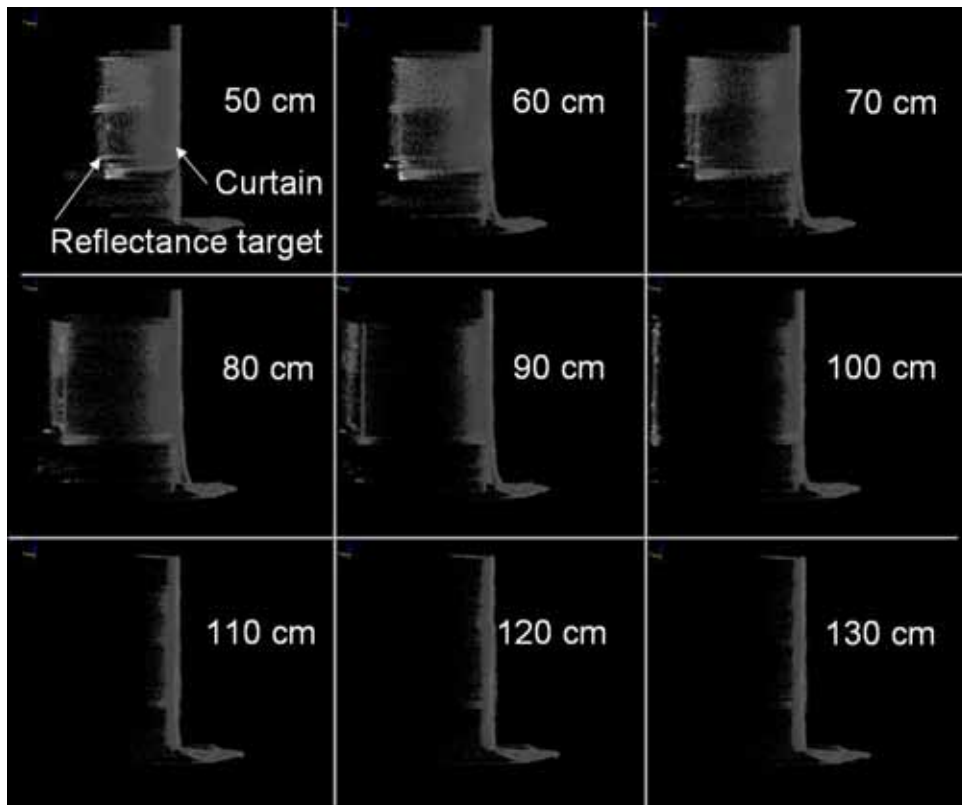


**Figure 23. Images showing the spread of ghost points between a curtain and reflectance target when the separation distance is changed.**

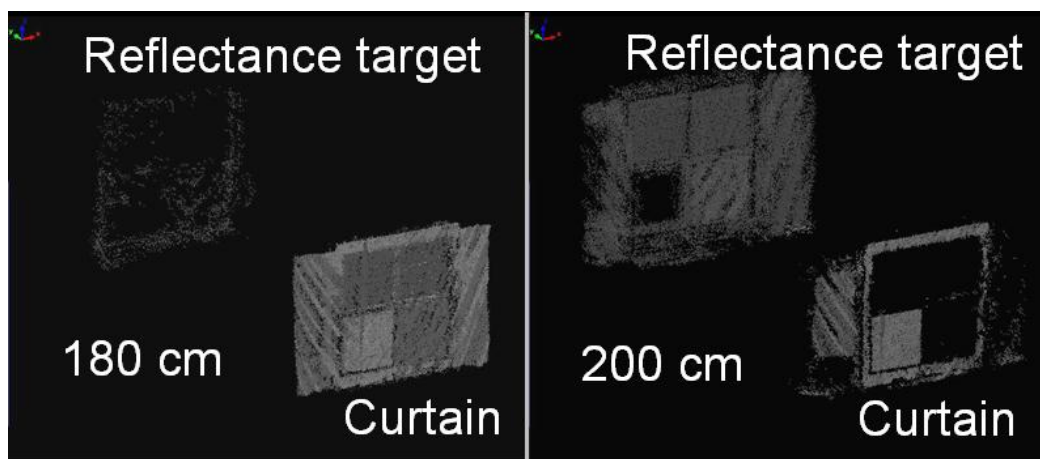


**Figure 24.** Image to left shows how most of the points are at the curtain when the separation distance is 180 cm and to the left, at 200 cm separation distance, most of the points are on the reflectance target.

## 7 3-D measurements and modeling.

Acquired data from ILRIS can be used to describe the 3-D world in different ways. Sometimes it is enough with just one acquired view to describe for instance a ground truth or data set used for further algorithm development. Figure 25 shows an example of a scene acquired from just one view. In this case it is enough to convert data to a readable format using the Parser software. Sometimes, however, more than one view is needed to cover a whole scene. These views can afterwards be stitched together. Figure 26 shows a nature scene stitched together from three views.

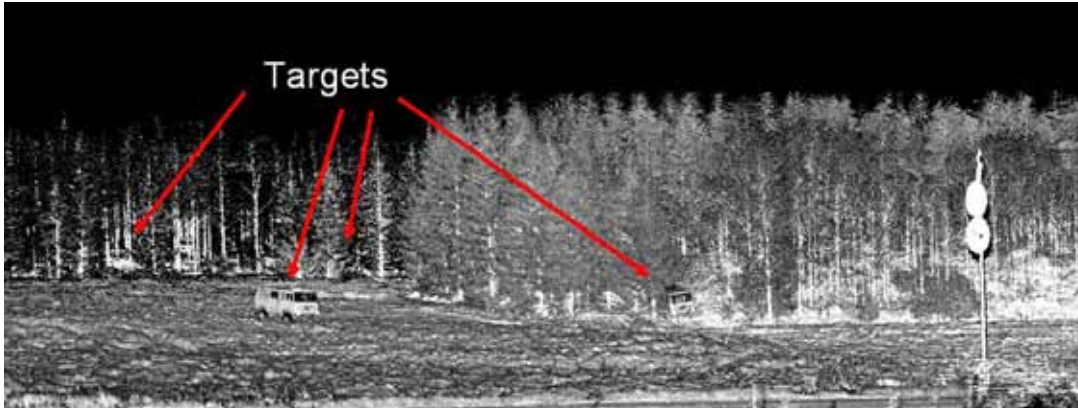


**Figure 25.** This is an example of a scene acquired from just one view.

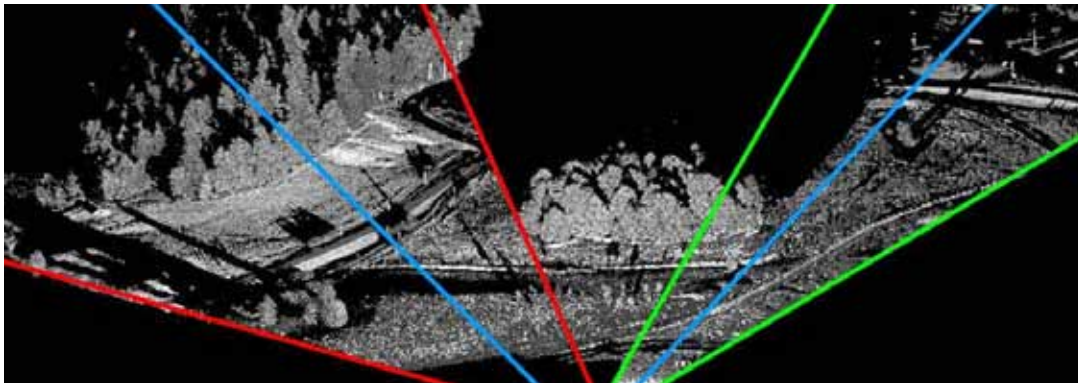


**Figure 26** Example of a scene acquired from three views; one view within each coloured pair of lines.

When acquiring data for a 3D-model (point cloud model or polygon model) there are two ways of working. One way is to let the object rotate and keep ILRIS in one position. Another way is to move ILRIS round the object and keep the object in one position.

To demonstrate how a 3d-model is built from scratch we will follow the modelling of a human. Several views of the person were acquired in increments of 45° and with ILRIS kept fixed in one position. The person was standing at a distance of 30m. Figure 27 shows the person in visual and an example of a 3-D view. We will later see that ILRIS has difficulty to resolve details in e.g. a face. Acquiring detailed data of a face is actually beyond the specification of ILRIS; however it is good enough for bigger constructions.



**Figure 27. Visual image to the left and to the right an intensity image from ILRIS. Notice the very low reflectance from human skin and the high reflectance from the clothes (from black to white in intensity the reflectance goes from low to high)**

### 7.1 PIFedit and PolyWorks

To build 3d-models from laser scanner data we use PolyWorks<sup>6,7</sup> from Innovmetric<sup>8</sup> in Canada. PolyWorks contains 7 modules (IMAlign, IMMerge, IMEdit, IMInspect, IMCompress, IMTexture and IMView) and also a detached program called PIFedit. PIFedit works with its own format pif as well as xyz. PolyWorks works with many point cloud formats as well as CAD formats. Many digitizers' data can be read in PolyWorks. FOI has a support and maintenance agreement with Innovmetric, which offers support at Innovmetrics website. Here a lot of tutorials and self study courses can be downloaded.

#### **PIFedit**

PIFedit is a detached program from PolyWorks program package. It is used for editing point clouds. Before a point cloud is used for modeling it is useful to remove points that are not supposed to be a part of the model. An example is shown in Figure 28, where points that will be removed and not used in further modeling are marked red. Masking of points is done for all acquired views.



**Figure 28. An example of a masked view in PIFEdit. Points marked in red will be removed.**

### **PolyWorks-IMAlign**

IMAlign is used to bring hundreds of scans into a common coordinate system, totaling tens of millions of points. IMAlign's main image alignment technique is an iterative algorithm that computes an optimal alignment by minimizing the 3-D distances between surface overlaps in a set of 3D images acquired from unknown viewpoints.

ILRIS has some recommended settings for the alignment procedures, see Figure 29:

- **Max angle (degrees).** The maximum angle between a surface normal vector and the  $z$  axis of the parameterized 3-D image coordinate system. This threshold is used to detect discontinuities in a 3-D image.
- **Max distance (m).** Acceptable maximum 3-D distance between two overlapping scans.
- **Convergence.** Defined as the sum of the squared differences between the identity matrix elements and the incremental matrix elements. To obtain fast and accurate results, the value of the Convergence parameter should be set to  $(\sigma/25)^2$ , where  $\sigma$  represents the standard deviation of the 3-D digitizer in model units. This guarantees that the accuracy of the final alignment will be at least 25 times better than the standard deviation of the 3-D imaging device.



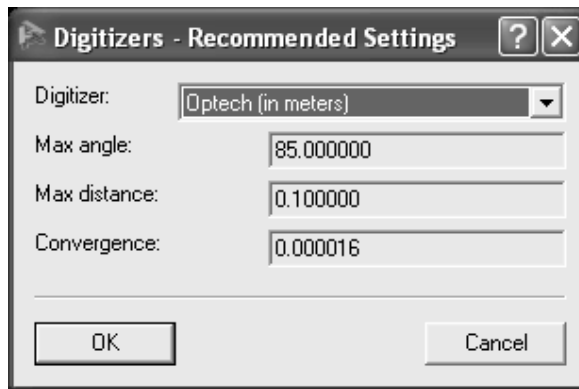


**Figure 29. Recommended setting for ILRIS for the alignment procedure.**

In Figure 30 two views are stitched together while defining at least three common points in these two views. After the alignment, the two views are locked to each other and a third view is aligned with the two first using the same procedure. The procedure is repeated until all acquired views has been aligned and locked to each other. The final point cloud is shown in Figure 31 from three directions. For further details about IMAlign see IMAlign reference manual<sup>9</sup>.

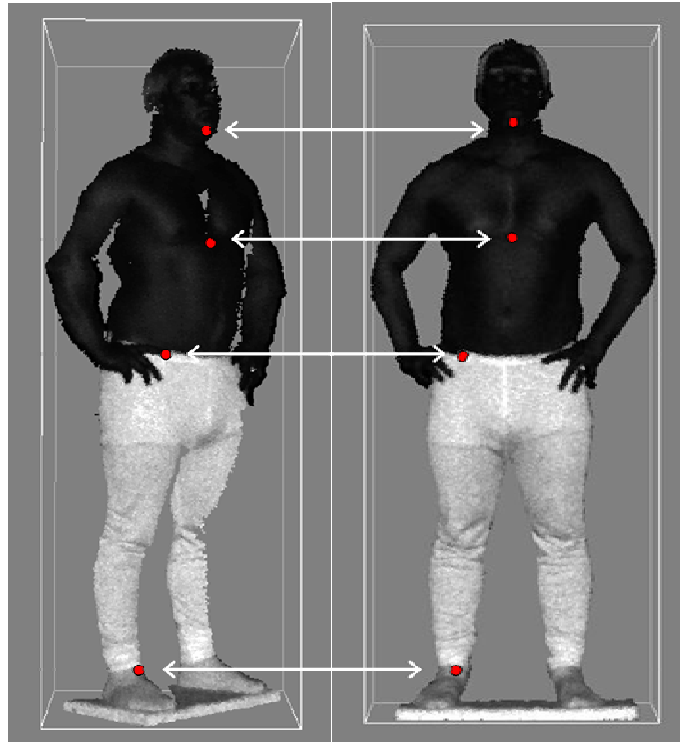


**Figure 30. At least three common points are chosen from two views.**

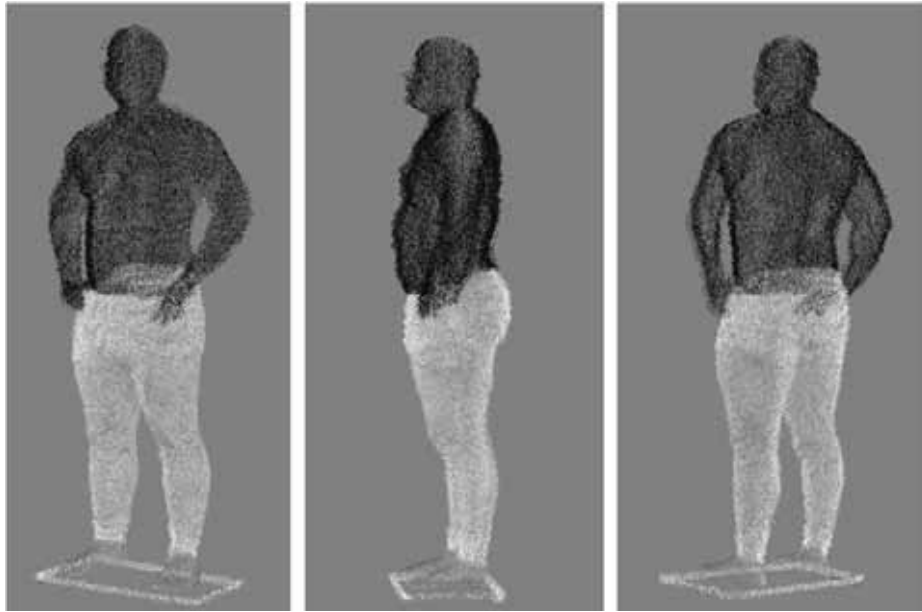


**Figure 31. The final aligned point cloud is here shown from three directions. The point cloud contains totally eight acquired and aligned views.**

### **PolyWorks-IMMerge**

IMMerge is a completely automated software tool for merging a set of aligned 3-D images into a global surface triangulation model. You can control triangle size, smooth the input data to remove digitizer noise, increasing the accuracy of your scanner data, and significantly reduce the model size

Figure 32 shows the model as it looks after merging but before editing. The noise in the model depends on ILRIS internal noise but also that the person has not been completely still during the data acquisition. For further details about IMMerge see IMMerge reference manual<sup>10</sup>.

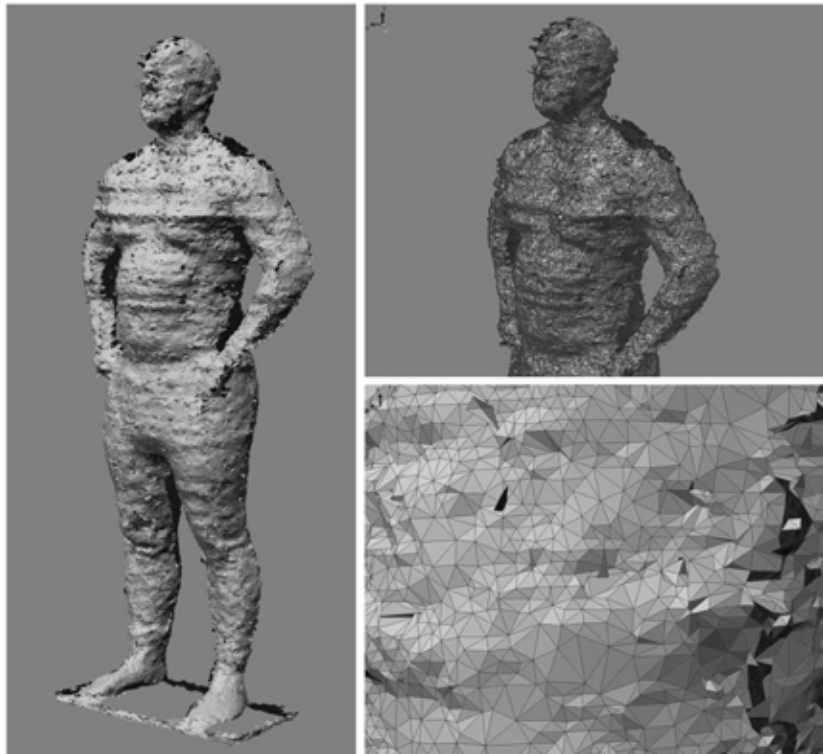


**Figure 32. The model before editing (hole filling, smoothing etc.). Lower right image shows how the triangles are built. The model contains triangles about 5 mm in size.**

### **PolyWorks-IMEdit**

IMEdit prepares the polygon model to fit further applications. IMEdit tool offers (some of all features):

- Fill holes
- Optimize the mesh
- Reconstruct edges, corners, and fillets
- Reduce the mesh
- Subdivide the mesh
- Smooth the mesh
- Trim the model etc.

The final model is shown in Figure 33. For further details about IMEdit see IMEdit reference manual<sup>11</sup>.

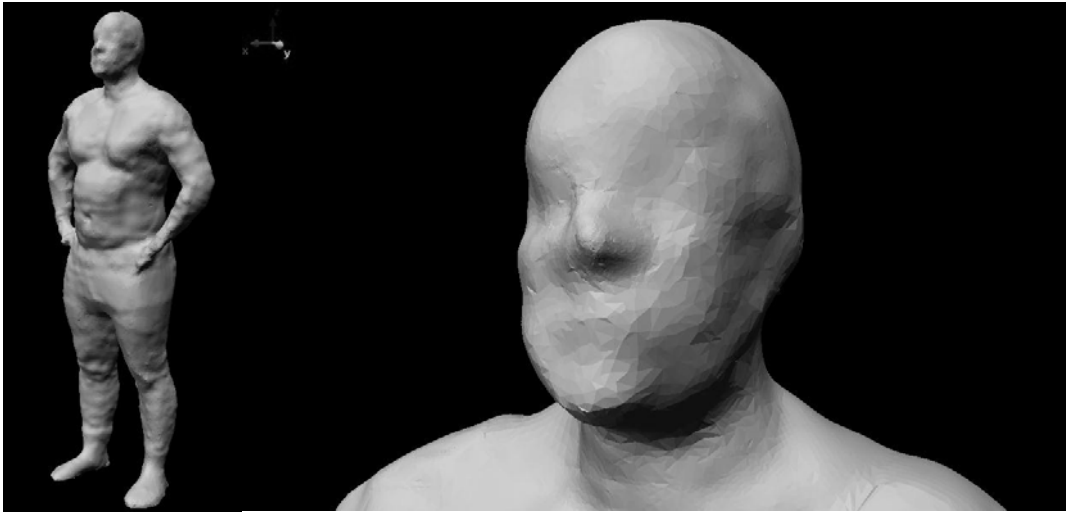


**Figure 33. The final model of a person, built from data acquired with ILRIS.**

### PolyWorks-IMInspect

IMInspect is a module for comparing data point clouds to reference surfaces, cross sections are used. There are many trigonometric features in the IMInspect module, volume calculations, measuring the dimensions of specific features such as distances, radius and angles etc. Figure 34 shows an example of deformation calculations using cross-sections and Figure 35 some examples of measurements of a vehicle.

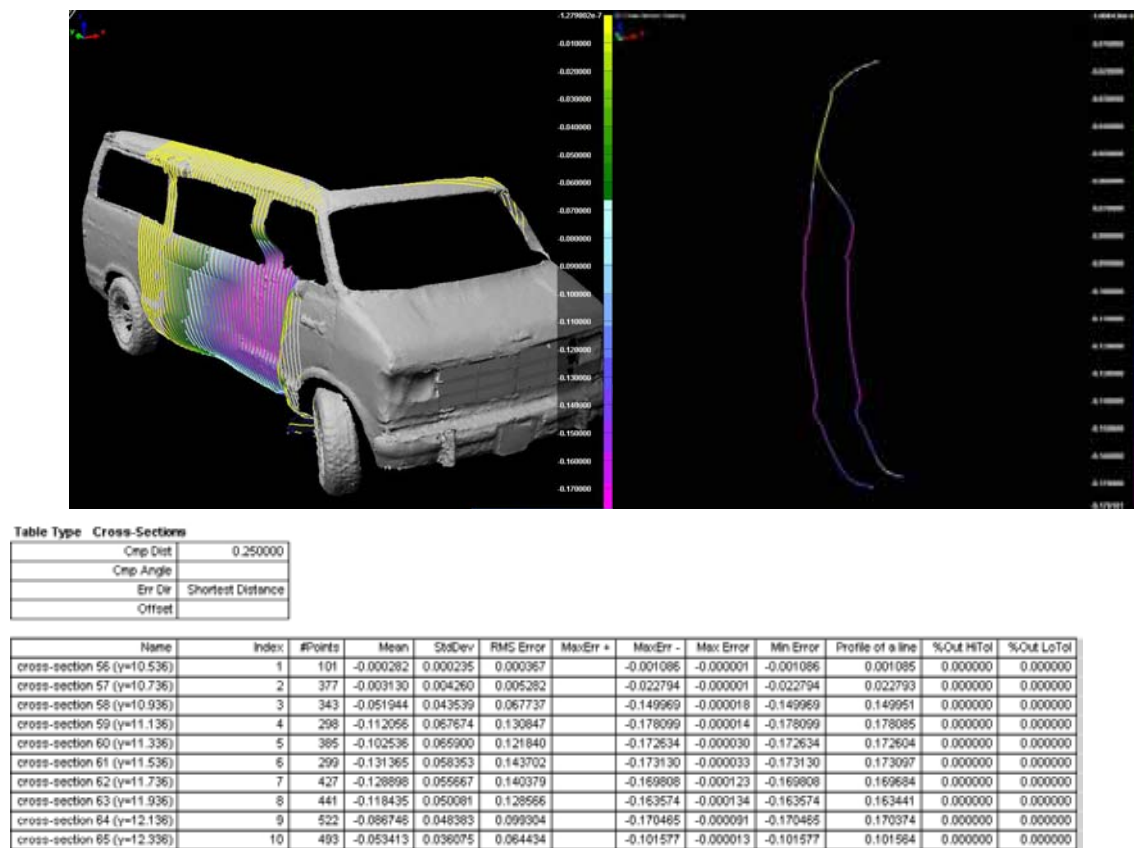


**Figure 34. Image illustrates a crashed van and how a deformation can be shown using “cross-sections”. The van is divided into 1 dm sections. The scale shows the deformation, where pink represents the largest deformation. In right image one specific cross-section has been chosen and compared to the origin. Cross-sections are presented in the table.**



**Figure 35. Image shows an example of some measurements made in the Inspect module. Survey measurement shows azimuth, bearing, and vertical angle of vehicles left side compared to scanner position. The lengths of the vehicle, the radius of the rim, the circumference of the grill are some other examples of measurements.**

IMInspect also offers tools for geo-reference. To geo-reference a data set, you need only three visible points in one scan, with the other scans overlapping, or three visible points in all the scans, with the scans aligned.

For further details about IMInspect see IMInspect reference manual<sup>12</sup>.

### **PolyWorks-IMCompress**

In the module IMCompress the polygon model can be compressed regarding number of surfaces or points. Figure 36 shows uncompressed model of a T72 tank containing 140000 surfaces, which has been compressed to 14000, 10000 and 8400 surfaces, respectively. You can see how the model starts to deform with decreasing number of surfaces. Limits can be set for compression regarding number of triangles and max edge lengths.

For further details about IMCompress see IMCompress reference manual<sup>13</sup>.

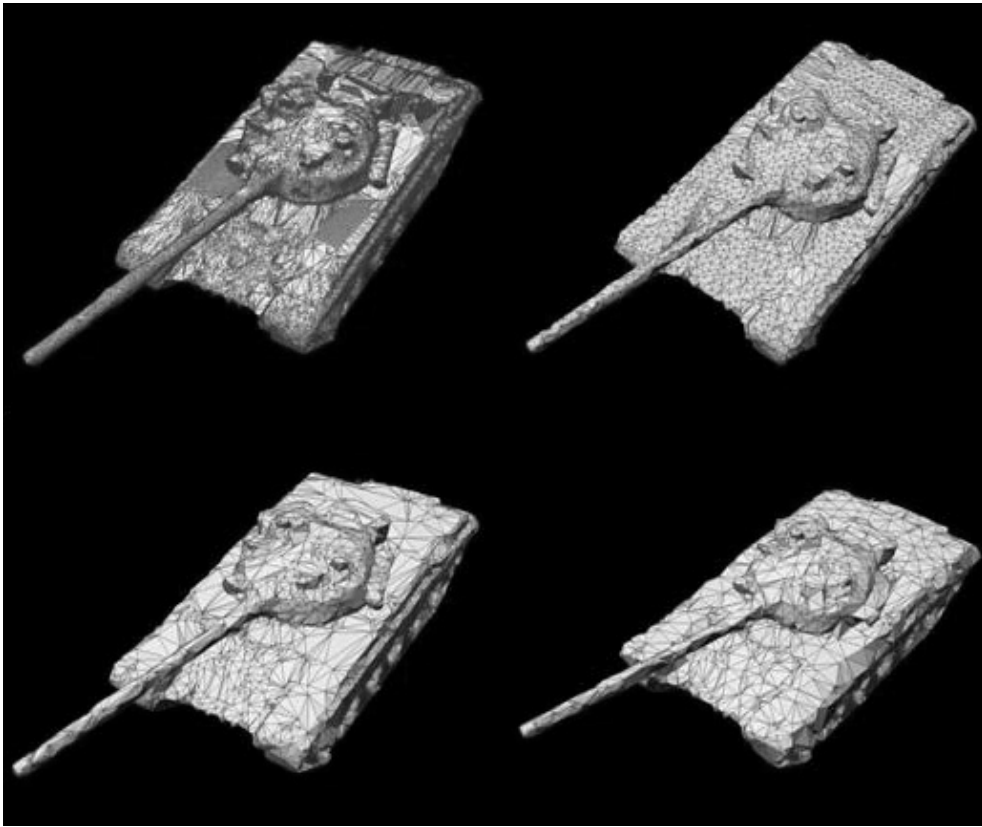


**Figure 36.** Image shows some compression grades of a model of a T72 tank. Upper left model contains 140000 triangle surfaces, upper right 14000 surfaces, lower left 10000 surfaces and lower right 8400 surfaces.

### **PolyWorks-IMView**

IMView is a free viewer that can be downloaded from Innovmetrics website. The viewer show polygon models and works with some different formats (\*.cnrc, \*.dxf, \*.nas, \*.obj, \*.ply, \*.pol, \*.pqk, \*.stl, \*.stla, \*.stlb, \*.wrl)

### **7.2 Texturing models**

ILRIS has an integrated video camera for the operator interface and for texturing the point cloud. Figure 37 shows a point cloud textured with both intensity values at 1541 nm and RGB-values from the integrated camera. Camera and laser are lined at about 80 meters. Tests show that it is hard to texture over shorter distances (shorter than 10 m) because of the parallax between camera and laser. The internal camera is good enough for texturing point clouds down to a resolution of 10 mm at 30m in distance. For a point cloud with higher resolution than that, an external camera should be used.



**Figure 37. The same point cloud textured with intensity at 1541 nm (left) and RGB (right).**

External camera can be mounted on the ILRIS handle with a mechanical adapter, see Figure 38 and the camera mounted in Figure 39. At present we use a Nikon D200 (10.2 Mega Pixels) as external camera, which is used to photo drape the point cloud. The Nikon camera has been calibrated at Optech together with ILRIS. Certain use of the Nikon D200 camera together with ILRIS must be obtained to maintain the calibration valid<sup>14</sup>. Calibration parameters are used together with the Parser and the software MatchView<sup>15</sup> to photo drape the point cloud. In the earlier software TexCapture, even meshed models in format VRML can be photo draped<sup>16</sup>. The external camera has a higher resolution (10.2 Mega Pixels) compared to the internal (6.6 Mega Pixels). Examples of texturing with images from an external camera are shown in chapter 7.2.

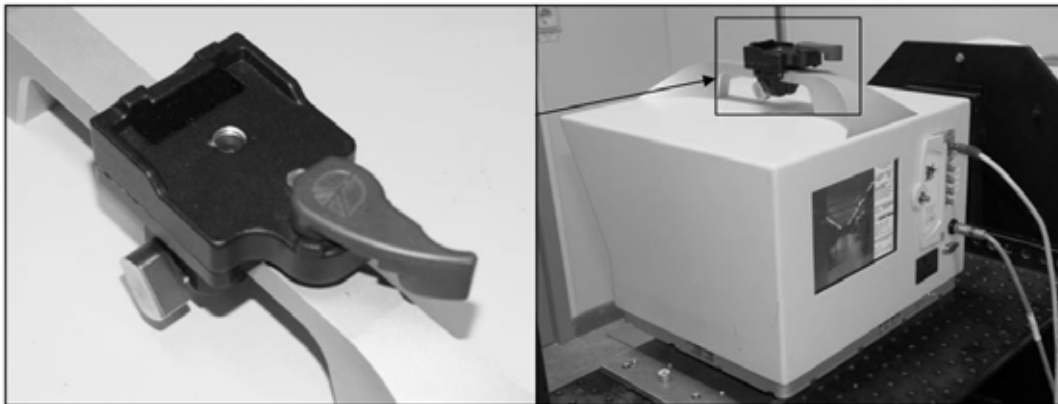


**Figure 38. Mount for external camera or GPS**



**Figure 39. External camera Nikon D200 mounted on ILRIS**

RGB-values can be set on each point in a cloud using the internal camera, or using an external camera. At every service occasion of ILRIS by Optech we have a camera calibration file delivered containing 15 parameters,

There are six external parameters:

- coordinates:  $X_c$ ,  $Y_c$ , and  $Z_c$  of the camera projection center,
- 3 rotations: pitch, roll, and yaw of the camera,

There are nine internal parameters:

- 1 camera focal length (or principal distance),
- 2 coordinates:  $x$  and  $y$  of the principal point (pp) of the image,
- 2 affine image parameters to correct for scale difference and non-perpendicularity of the  $x$  and  $y$  image coordinates,
- 2 radial lens distortion parameters (third and fifth order),
- 2 decentering lens distortion parameters.

The file has however 19 rows and is built as follows:

- 1 – number of 2D picture (s)
- $X_c$  – position of the camera in the ILRIS coordinate system
- $Y_c$  – position of the camera in the ILRIS coordinate system
- $Z_c$  – position of the camera in the ILRIS coordinate system
- Pitch
- Yaw
- Roll
- Focal Length
- $X_o$  – principle offset
- $Y_o$  – principle offset



- affine1
- affine2
- radial 3rd
- radial 5th
- decentering lens distortion 1
- decentering lens distortion 2
- 1 – ratio between calibration units and 3D data
- Pixel Size X
- Pixel Size Y

The camera calibration file can be used in the Parser software to immediately texture a point cloud. Under Color Channel “Use External Texture & Parameter File” must be marked and camera calibration file must be choose under Texture Calibration Parameter File

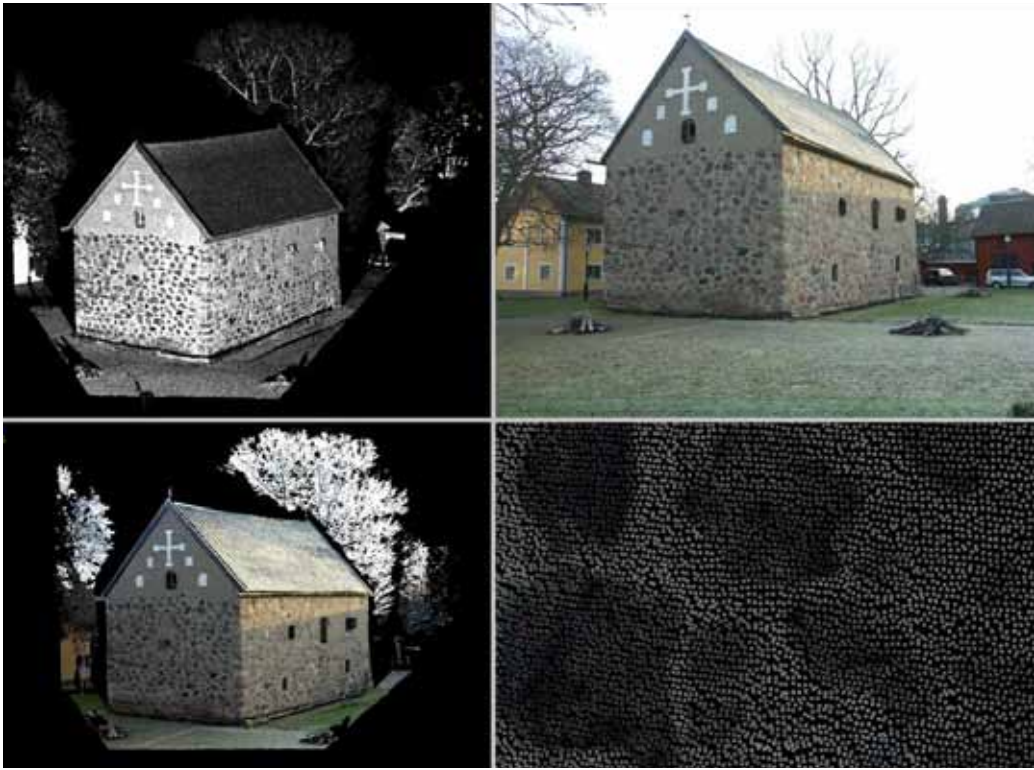
Optechs software Matchview<sup>15</sup> is used for photo draping point clouds. TexCapture<sup>16</sup> can be used for calibration of internal and/or external camera but also for photo draping polygon models.

Figure 40 shows an example of a church with a draped photo.



**Figure 40. Photo draping of a church. Polygon model to the left and visual photo in the middle are fused together to a photo draped model to the right. (Data and photo from Optech.)**

For a point cloud with a resolution better than one cm over a distance of 30 m the external camera should be used for draping the cloud. FOI has developed a method for draping high resolution point clouds using Matlab. Figure 41 shows such draping.



**Figure 41** Point cloud textured with an external photo. Intensity point cloud upper left. Upper right shows a visual photo from external camera. Lower left textured point cloud and lower right shows the RGB point cloud enlarged.

TexCapture offers a complex way of calibrating cameras using a very complex calibration arrangement; see Figure 42 for an optimal suggestion. All reference targets must have a unique specified coordinate (accuracy better than 1mm).

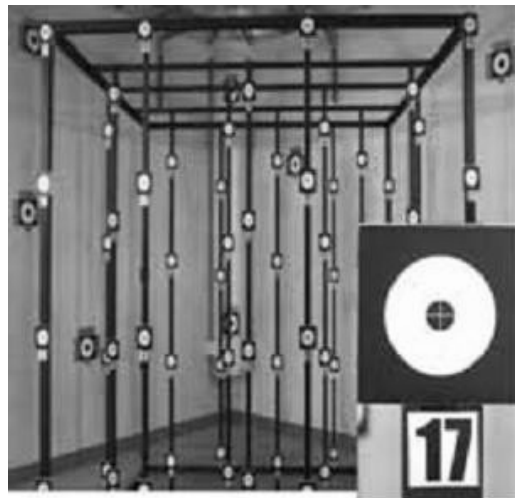


**Figure 42.** Optimal camera calibration arrangement for the TexCapture software.

To avoid a complex calibration arrangement with the need for targets with unique coordinates, PhotoModeler is software that uses a simpler arrangement. PhotoModeler use a target with 100 points in a pattern that is mutual specified. The dimension of the target is not important as long as the pattern is the same. As can be seen in Figure 43, there is one symbol in each corner that PhotoModeler use to for automatic calibration. The calibration work flow will be described in a future report.

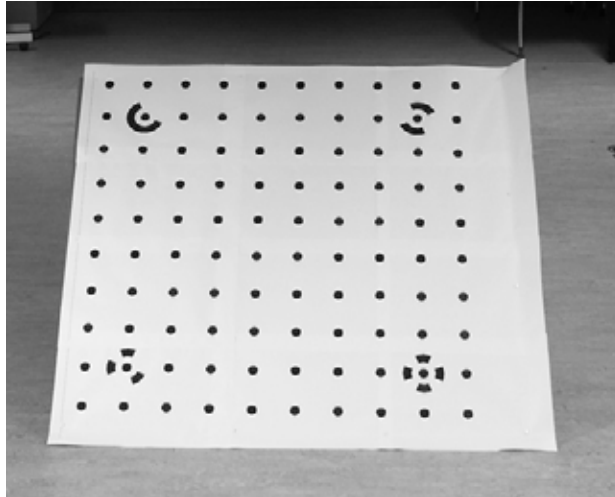


**Figure 43. Target to use together with the PhotoModeler program**

## 8 Reflectance information from intensity data

ILRIS is not intended for measuring intensity other than for good visualizations. We have however developed a method to calculate the reflectance information from ILRIS intensity data. Here, we use a reflectance target, with calibrated reflectance for the 1550 nm wavelength, to transform measured intensity to reflectance.

### 8.1 Reflectance target

When acquiring data for reflectance calculations we must have a reflectance target in within the view to be able to convert the intensity to reflectance, but also because of nonlinear presentation of intensity and the problem to reproduce intensity because of temperature variations, see chapter 6. The reflectance target consists of 8 reflectance surfaces, see Figure 44, and each surface has been calibrated with 8°/Hemispherical Spectral Reflectance factor. The surfaces are Lambertian with values reflectance 1.7 %, 3.2 %, 6.0 %, 15.6 %, 29.0 %, 48.8 %, 61.9 %, and 98.8 %, respectively. Four of the surfaces are manufactured from Labsphere (1.7 %, 29.0 %, 61.9 % and 98.8 %) and the other four have been manufactured at FOI using white and black Nextel colours which have been mixed to four nuances.

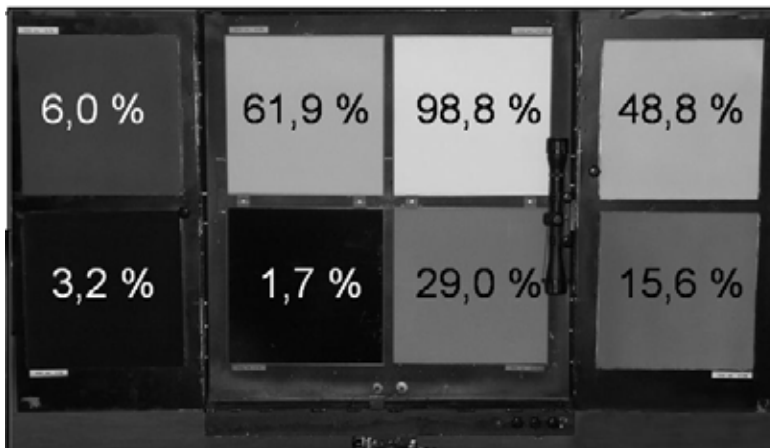


**Figure 44. Reflectance target with eight surfaces. Values are calibrated reflectance values at 1550nm.**

We have checked if the surfaces are indeed Lambertian (ideally diffuse); i.e. follow an ideal cosine. All surfaces were measured from 0° up to at least 70°. For the targets from Labsphere we can see in Figure 45 that the surfaces follow an ideal cosine fairly well. For the FOI manufactured surfaces, see Figure 46, we can see that the 6 % and 15.6 % surfaces do not decrease as fast as they should.

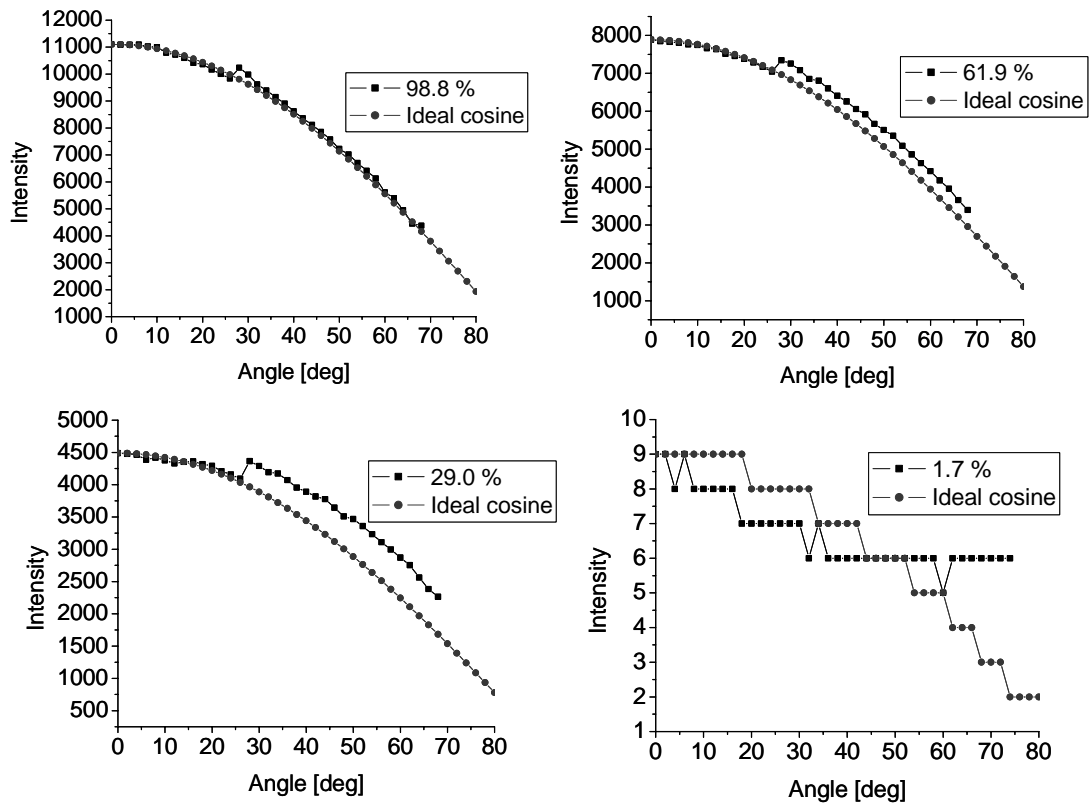


**Figure 45.** The surfaces from Labshere follow an ideal cosine fairly well. (The increasing value we see at 26 degrees depends on a break in the acquirement and ILRIS was warmed up which affected the intensity value)

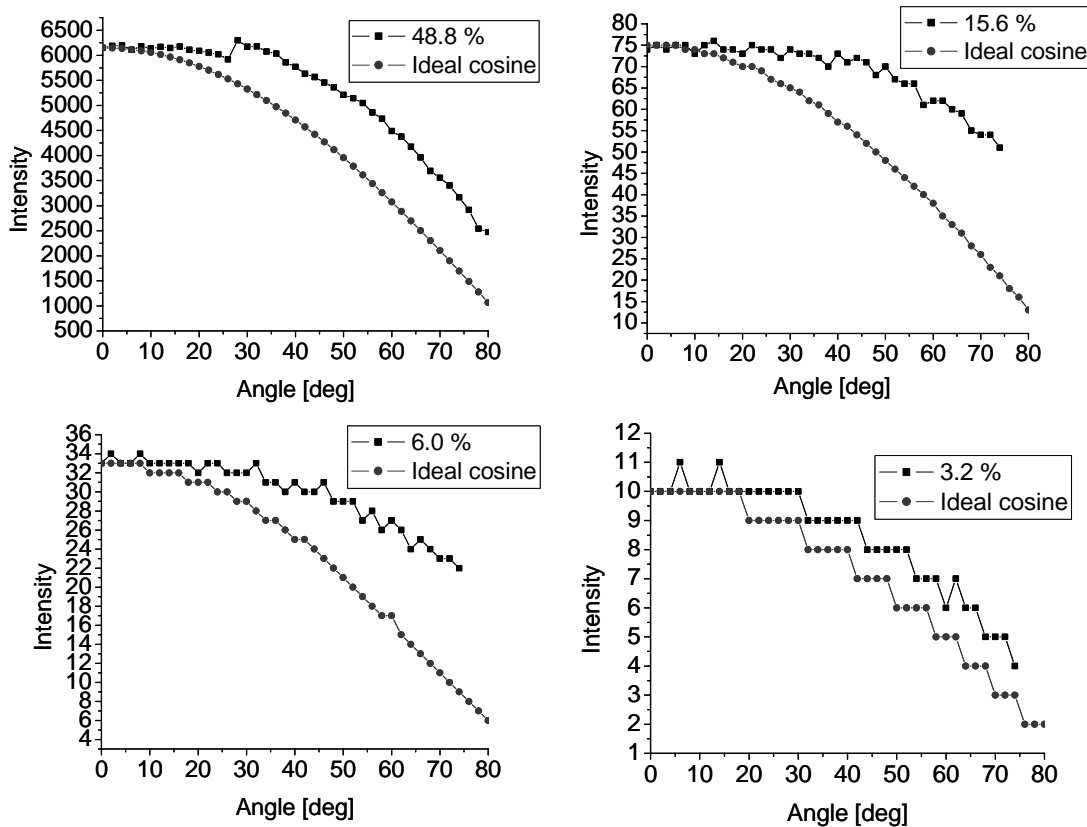


**Figure 46. The angular reflectance of the FOI manufactured surfaces follows an ideal cosine (ideal diffuse) fairly well. We can however see for 6.0 % and 15.6 % that the values don't decrease as fast as it should. (The increasing value we see at 48.8 % surface at 26 degrees depends on a break in the data acquisition and ILRIS was warmed up which affected the intensity value)**

## 8.2 ILRIS presentation of intensity over the distance

Intensity measurements at varying distance shows a nonlinear behaviour, see Figure 47. Each intensity value is a mean, containing hundreds of points. Intensity values measured within 10 meters in distance are saturated and are therefore not useful for reflectance calculations. Notice also the knee for all curves when passing through low to high gain at 255 digits. We can see how the intensity value starts to level at 300 digits which depends on values both in high and low gain (gain difference, factor 100). As a rule of thumb, try to avoid acquiring intensity data represented in both gain domains when doing reflectance measurements. A look at the intensity data in a pre-scan can show if the distance is right for the intensity data of measured object to be within one gain domain. As can be seen in the graph in Figure 47 a target range distance exceeding 35 m ensures the high gain domain, at least for reflectance values below 29 %

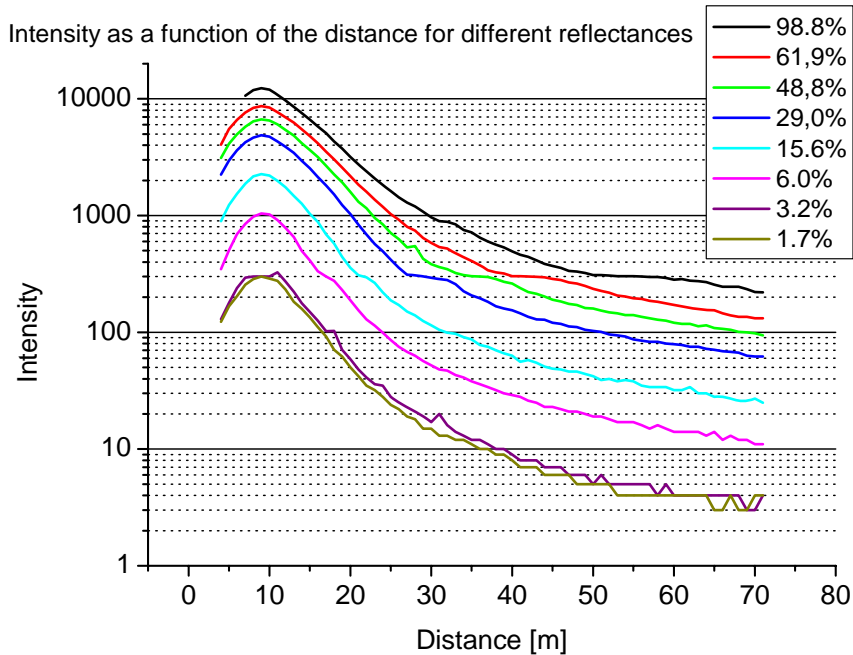


**Figure 47.** The measured intensity as a function of the distance for eight different reflectance surfaces.

### 8.3 Method for reflectance calculations

The LabVIEW application ScanView has been used to evaluate the reflectance. Scan View has been developed by FOI. In the Scan View application, the intensity and range can be read and the reflectance and laser cross sections can be calculated. The raw format (\*.raw) is used for the ScanView application. The point cloud is presented as a bitmap picture, with the point cloud x- and y-coordinates. Z coordinates and corresponding intensities can be read from the raw file knowing the x- and y-coordinate, see Figure 48.

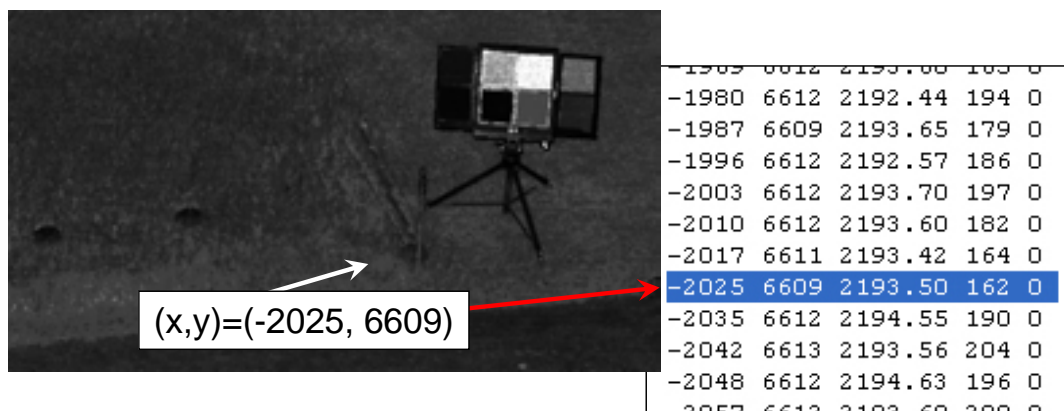


**Figure 48.** The x- and y-coordinate in the bitmap is found in the raw text file in behind where the corresponding z-coordinate and intensity value can be read.

A region of interest can be set in the bitmap as  $x$  and  $y$  coordinates. The distance and intensity of every point in the selected region can then be read. ILRIS has a very nonlinear intensity response; see Figure 47. The nonlinearity can be described for each reflectance surface  $i$  by

$$S = k_i R^{x_i} \quad (3)$$

where  $S$  is the intensity,  $k_i$  is a constant,  $R$  is the range, and  $x_i$  is the exponent. Notice that the equation is only valid in a specified range interval where all points will be distance compensated in intensity. For each reflectance target the exponent  $x_i$  must be calculated. This is easiest done in Excel where a trend line of an exponent equation is calculated, see Figure 49 which is the 29.0 % reflectance target values from Figure 47 between 40 to 60 m. In this example the calculated equation gives a decrease in intensity  $y$  by a factor  $1/x^{1.619}$ , where  $x$  is the distance. For calibrating each reflectance target to a mean intensity value of all point inside a region, a region of interest (ROI) is defined in the bitmap, see Figure 50.

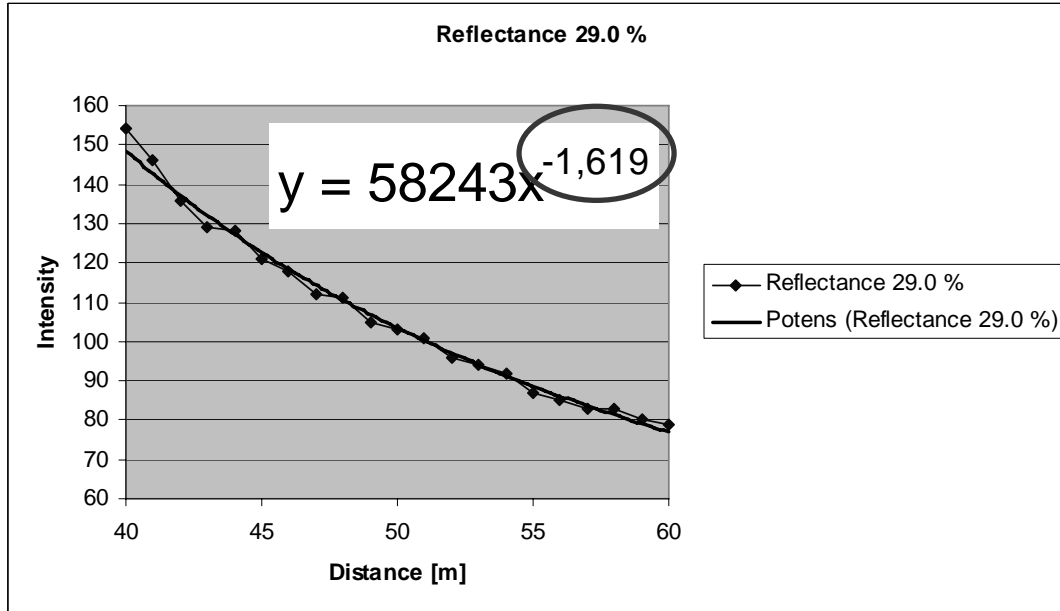


**Figure 49.** Calculation of an exponent valid for the 29.0 % reflectance target between 40 and 60 m.

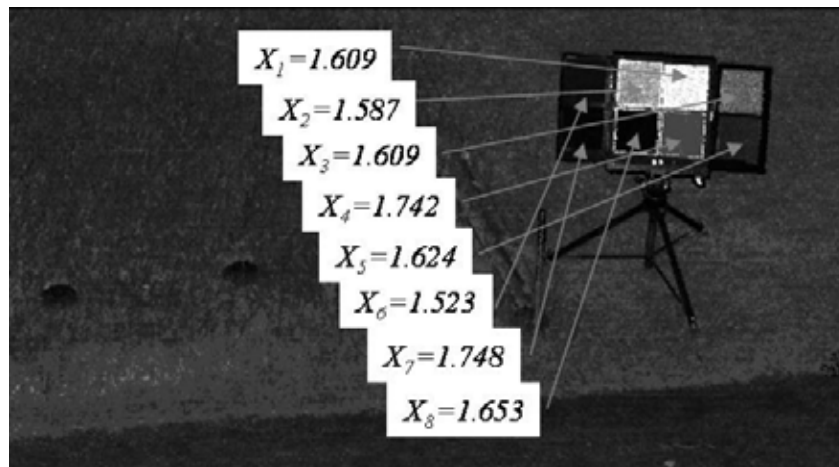


**Figure 50.** An exponent for every reflectance surface is calculated and used as parameters to ScanView.

In every data set (intensity image; bitmap), the calibrated reflectance surfaces (intensity value and range) have been read. Knowing the distance to and the intensity of both the reference target and every point in the point cloud, a distance compensation for every point can be made according to



$$S_{tarcomp} = S_{tar} \cdot \frac{R_{ref}^{x_i}}{R_{tar}^{x_i}} \quad (4)$$

where  $S_{tarcomp}$  is the range-compensated intensity value;  $S_{tar}$  is the measured intensity for this single point;  $R_{ref}$  the mean distance to the reference surface;  $R_{tar}$  is the distance to this single point; and  $x_i$  is the exponent indexed to each reflectance surface. The exponent value depends on the intensity value and the range of the target. The compensated intensity value is compared with the intensity values on the reference reflectance surfaces. Every reflectance surface will be described by its own linear equation. The intensity values from the reflectance surfaces are used as interval limits when the linear equation

$$\rho_{tar} = K_i \cdot S_{tarcomp} + M_i \quad (5)$$

is used for to calculate the reflectance with linear regression. Here,  $\rho_{tar}$  is the reflectance for each point,  $i$  is the index for the intensity limits taken from the reflectance surfaces, and  $K_i$  and  $M_i$  are the regression constants.

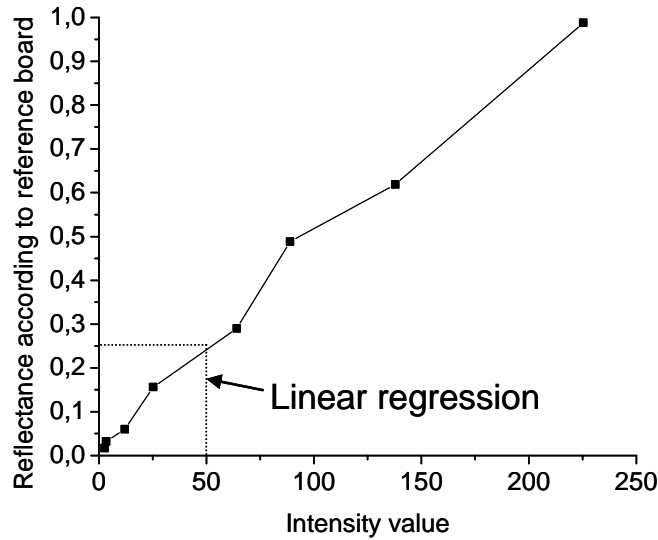


**Figure 51. Graph of reflectance according to reference surface as a function of intensity. For each point the reflectance is calculated using linear regression. In this example, an intensity value of 50 corresponds to a reflectance of 0.25.**

#### 8.4 Error analysis of calculated reflectance

This error analysis is an example from a data set from an intensity calibration where the reflectance surfaces were placed at a distance of 30 m.

For the reflectance calculations we use the distance and the intensity data. We have earlier showed that the distance data has a good accuracy around 8 to 10 mm. We also know the quantization

error for the intensity is 0.5 units for all values in high gain and 50 in the low gain area. We use a reflectance target with 8 calibrated reflectance values. The calibration method gives an uncertainty of 2 % of the absolute value, see Table 5. The table also shows mean intensity value and standard deviation for the intensity at each reflectance surface.

**Table 5 Measured mean intensity and standard deviation for reference surfaces.**

Reflectance value* [%]	Std dev** reflectance +1 Sigma	Std dev** reflectance -1 Sigma	No of points	Mean intensity value	Std dev** intensity +1 Sigma	Std dev** intensity -1 Sigma
0,988	1,008	0,968	656	967,91	1088,97	846,85
0,619	0,631	0,607	553	585,90	677,67	494,11
0,488	0,498	0,478	496	382,86	452,26	313,46
0,29	0,296	0,284	425	296,43	312,21	280,65
0,156	0,159	0,153	473	115,26	132,09	98,43
0,06	0,061	0,059	379	52,058	58,76	45,35
0,032	0,032	0,031	295	17,342	19,83	14,84
0,017	0,017	0,017	265	14,174	17,16	11,18

\*Lambert surfaces

\*\* $k=1$  for the reflectance and intensity, which for a normal distribution means 68 % of all points is within the intensity value  $\pm 1$  standard deviation.

Below the lowest value ( $\rho_{\text{Lambert}}$ ) of reflectance target of 1.7% we have to assume that 0 in intensity is 0 in reflectance. We extrapolate points between 1.7 % down to 0.

Very often we calculate the reflectance from measurements where the reflectance surfaces and interesting targets (backgrounds for instance) are at the same distance, within a couple of decimeters. Then assume that all target points are at the same distance as the reference surfaces (no distance compensation needed). The values in Table 5 have been used in the linear equation (5), one for plus one standard deviation and one for minus one standard deviation. We will get a relative error of absolute value as presented in Figure 52.

The relative error is mostly below 20 %. The rather high error in the lower reflectance regions depends on both a high standard deviation at the two lowest reflectance surfaces and a very small dynamic presentation between these two surfaces. A small change of intensity in the lower intensity area makes a big change in the reflectance, which causes a great error.

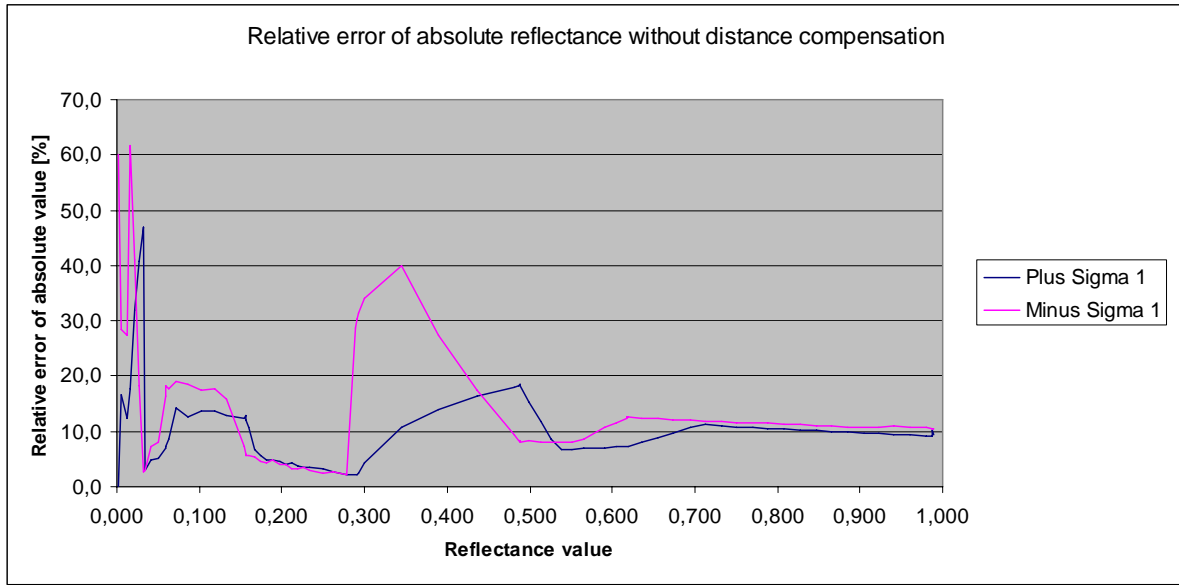


**Figure 52. Relative reflectance error in percent of the absolute value.**

### 8.5 Calculation of laser cross section of a target

ScanView is also used for calculating the laser cross section of an object. As mentioned before, the angle resolution can be choose as multiples of  $26.6 \mu\text{rad}$  in 100 steps.

Every laser pulse illuminates an area on the target,  $Area_{spot}$ , according to

$$Area_{spot} = (\tan \alpha_{spot} \cdot Z)^2 \text{ [m}^2\text{]} \quad (6)$$

The total laser cross section  $A_{\Delta}$  is calculated as

$$A_{\Delta} = \frac{\rho_m \cdot \Sigma A_{spot}}{\pi} \text{ [m}^2\text{/sr]} \quad (7)$$

where  $\rho_m$  is the mean value of all points reflectance value calculated from (5) and  $\Sigma A_{spot}$  is the sum of all areas calculated from (6).

To calculate the laser radar cross section of an object in a scene, a mask of the bitmap image (the intensity image of the scene) is produced in Photoshop, where all uninteresting points are set to black and the pints to keep are set to white. In this example, we use the scene from Figure 48 showing the reflectance target.

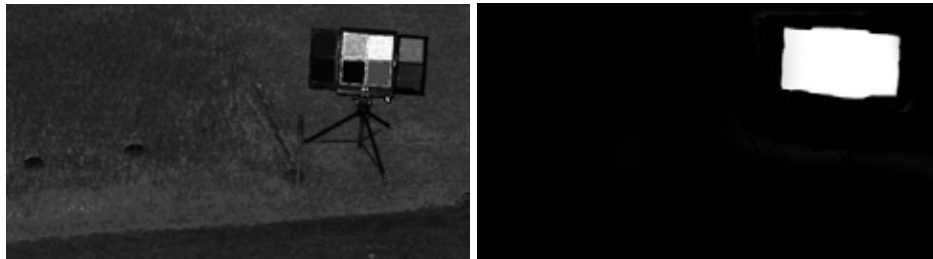


**Figure 53. Image to the right shows a mask of the intensity view to the left. The laser radar cross section will only be calculated from points separated from black (in this case the reflectance target).**

The calculated laser radar cross section value will depend on the angle of incidence to the object. The calculated laser cross sections of all acquired angles are afterwards presented in a polar plot.

## 9 Measurements from the analogue outputs

As mentioned in chapter 4.1, an extra feature of analogue outputs are installed in our ILRIS. This makes it possible to acquire the full waveform of the return signal. There are four analogue outputs:

- Laser trigger
- Line trigger
- Detector signal high gain
- Detector signal low gain

All signals are low impedance ( $50\Omega$ ). We use the laser trigger as a trigger for the oscilloscope. Depending on the signal amplitude, high or low gain is chosen.

The laser is pulsing with 2 kHz when power is on. The galvanometer mirrors are standing in one position. The easiest way to have control of the position is to have ILRIS mounted at our MicroControl turn table and use an InGaAs camera to monitor where the laser is pointing.

Figure 54 shows the measurement performance with ILRIS mounted on the turntable.

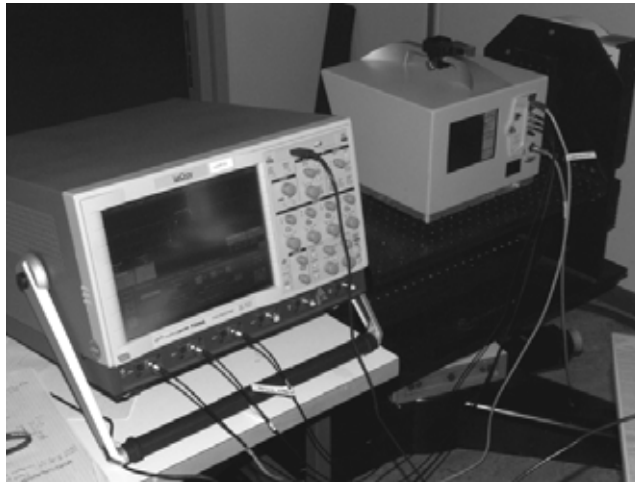


**Figure 54. Waveform acquisition using the analogue outputs. ILRIS is mounted on a Micro Control turn table to have control of the beam without scanning the galvanometer mirrors.**

## 10 References

- 
- <sup>1</sup> [www.optech.ca](http://www.optech.ca) ; Optech Incorporated, 300 Interchange Way, Vaughan, ON, Canada L4K 5Z8, Tel: (905) 660-0808
  - <sup>2</sup> [www.antonbauer.com](http://www.antonbauer.com)
  - <sup>3</sup> ILRIS-3D Operational Manual, 290000602/RevE, August 2005
  - <sup>4</sup> ILRIS-3D Survey Guide, document No. 0000000/Rev A, June 2005 (iPAQ)
  - <sup>5</sup> ILRIS-3D Survey Guide, document No. 0000000/Rev A, June 2005 (PC)
  - <sup>6</sup> PolyWorks, Modelling & Inspection Software Suite for 3D Digitizers, Reference Guide Version 9.1 for Windows, April 2006, 155 p.
  - <sup>7</sup> PolyWorks V9 Beginners Guide, May 2005
  - <sup>8</sup> [www.innovmetric.com](http://www.innovmetric.com)
  - <sup>9</sup> PolyWorks/IMAlign, Multiple 3D Images Alignment Software, Reference Guide Version 9.1 for Windows, March 2006, 206 p.
  - <sup>10</sup> PolyWorks/IMMerge, Multiple 3D Images Merging Software, Reference Guide Version 9.1 for Windows, March 2006, 24 p.
  - <sup>11</sup> PolyWorks/IMEdit, Polygon-editing software, Reference Guide Version 9.1 for Windows, March 2006, 450 p.
  - <sup>12</sup> PolyWorks/IMInspect, Comparison and Verification Software, Reference Guide Version 9.1 for Windows, April 2006, 765 p.
  - <sup>13</sup> PolyWorks/IMCompress, Polygon Reduction Software, Reference Guide Version 9.1 for Windows, March 2006, 28 p.
  - <sup>14</sup> Camera Calibration Nikon D200 instruction.doc, unregistered document.
  - <sup>15</sup> ILRIS-3D Matching Viewer Guide 0041462/RevA, document delivered in the software
  - <sup>16</sup> A guide to Using Optech TexCapture, document delivered in the software

## Address to Optech Incorporated

Optech Incorporated  
 300 Interchange Way  
 Vaughan, Ontario  
 Canada, L4K 5Z8

Tel: 1-905-660-0808  
 Fax: 1-905-660-0829

## Contact persons at Optech

<b>Name</b>	<b>Main task</b>	<b>email</b>
Colin Young Pow	Software Applications Specialist	<a href="mailto:coliny@optech.ca">coliny@optech.ca</a>
Brad Ysseldyk	Regional Sales Manages	<a href="mailto:brady@optech.ca">brady@optech.ca</a>
Albert Iavarone	Product Manager	<a href="mailto:alberti@optech.ca">alberti@optech.ca</a>
Chric Verheggen	Engineering Manager	<a href="mailto:chrisv@optech.ca">chrisv@optech.ca</a>
Judith Mariampillai	GIS Application Specialist	<a href="mailto:judithm@optech.ca">judithm@optech.ca</a>
Brent W. Gelhar	Director	<a href="mailto:brentg@optech.ca">brentg@optech.ca</a>
Shana Albo	Sales & Repairs Administrator	<a href="mailto:shanaa@optech.ca">shanaa@optech.ca</a>

Comments: Colin Young-Pow is best to contact when having problem with ILRIS. He will contact the right person who will come back to us. Brad Ysseldyk is best to talk to when buying things from Optech. Shana Albo is the person who takes care about delivery to and from Optech.

Spatial resolution [m] at various distances for  
different spot step settings (SS)

APPENDIX B

Distance [m]	SS1	SS2	SS3	SS4	SS5	SS6	SS7	SS8	SS9	SS10
10	0,0003	0,0005	0,0008	0,0011	0,0013	0,0016	0,0019	0,0021	0,0024	0,0027
20	0,0005	0,0011	0,0016	0,0021	0,0027	0,0032	0,0037	0,0043	0,0048	0,0053
30	0,0008	0,0016	0,0024	0,0032	0,0040	0,0048	0,0056	0,0064	0,0072	0,0080
40	0,0011	0,0021	0,0032	0,0043	0,0053	0,0064	0,0075	0,0085	0,0096	0,0107
50	0,0013	0,0027	0,0040	0,0053	0,0067	0,0080	0,0093	0,0107	0,0120	0,0133
60	0,0016	0,0032	0,0048	0,0064	0,0080	0,0096	0,0112	0,0128	0,0144	0,0160
70	0,0019	0,0037	0,0056	0,0074	0,0093	0,0111	0,0130	0,0148	0,0167	0,0185
80	0,0021	0,0043	0,0064	0,0085	0,0107	0,0128	0,0149	0,0170	0,0192	0,0213
90	0,0024	0,0048	0,0072	0,0096	0,0120	0,0144	0,0168	0,0192	0,0216	0,0240
100	0,0027	0,0054	0,0081	0,0108	0,0135	0,0162	0,0189	0,0216	0,0243	0,0270
150	0,0040	0,0080	0,0120	0,0160	0,0200	0,0240	0,0280	0,0320	0,0360	0,0400
200	0,0053	0,0107	0,0160	0,0214	0,0267	0,0321	0,0374	0,0428	0,0481	0,0533

Distance [m]	SS20	SS30	SS40	SS50	SS60	SS70	SS80	SS90	SS100
10	0,0053	0,0080	0,0107	0,0133	0,0160	0,0186	0,0213	0,0240	0,0266
20	0,0107	0,0160	0,0213	0,0266	0,0320	0,0373	0,0426	0,0479	0,0533
30	0,0160	0,0240	0,0320	0,0400	0,0480	0,0560	0,0640	0,0720	0,0800
40	0,0213	0,0320	0,0426	0,0533	0,0639	0,0746	0,0852	0,0959	0,1065
50	0,0266	0,0399	0,0532	0,0665	0,0798	0,0931	0,1064	0,1197	0,1332
60	0,0320	0,0480	0,0640	0,0800	0,0960	0,1120	0,1280	0,1440	0,1600
70	0,0373	0,0561	0,0748	0,0936	0,1124	0,1311	0,1499	0,1687	0,1874
80	0,0426	0,0639	0,0852	0,1065	0,1278	0,1491	0,1704	0,1917	0,2130
90	0,0480	0,0720	0,0960	0,1200	0,1440	0,1680	0,1920	0,2160	0,2400
100	0,0540	0,0810	0,1080	0,1350	0,1620	0,1890	0,2160	0,2430	0,2700
150	0,0800	0,1200	0,1600	0,2000	0,2400	0,2800	0,3200	0,3600	0,4000
200	0,1065	0,1598	0,2127	0,2659	0,3190	0,3721	0,4253	0,4784	0,5315

Spot step	Full FOV (40°x40°)	Half FOV (40°x20°)	¼ FOV (20°x20°)	1/8 FOV (20°x10°)	1/16 FOV (10°x10°)	1/32 FOV (10°x5°)
SS1	104:59:15	52:29:47	26:15:01	13:07:38	06:33:57	03:17:07
SS2	26:15:00	11:54:48	06:33:56	03:17:08	01:38:40	00:49:28
SS3	11:39:58	05:50:12	02:55:13	01:27:44	00:44:00	00:22:07
SS4	06:33:59	03:17:07	01:38:41	01:03:15	00:24:52	00:12:33
SS5	04:12:13	02:06:14	01:03:15	00:31:45	00:16:00	00:08:07
SS6	02:55:13	01:27:44	00:44:00	00:22:07	00:11:11	00:05:43
SS7	02:08:48	01:04:32	00:32:23	00:16:19	00:08:17	00:04:16
SS8	01:38:40	00:49:28	00:24:51	00:12:33	00:06:24	00:03:20
SS9	01:17:59	00:39:08	00:19:42	00:09:58	00:05:07	00:02:41
SS10	01:03:15	00:31:45	00:16:00	00:08:08	00:04:11	00:02:13
SS20	00:15:59	00:08:07	00:04:11	00:02:13	00:01:14	00:00:45
SS30	00:07:13	00:03:45	00:02:00	00:01:07	00:00:41	00:00:28
SS40	00:04:11	00:02:13	00:01:14	00:00:45	00:00:30	00:00:22
SS50	00:02:45	00:01:30	00:00:53	00:00:34	00:00:24	00:00:20
SS60	00:01:59	00:01:07	00:00:41	00:00:28	00:00:22	00:00:18
SS70	00:01:22	00:00:49	00:00:32	00:00:23	00:00:19	00:00:17
SS80	00:01:13	00:00:44	00:00:30	00:00:22	00:00:19	00:00:17
SS90	00:01:01	00:00:38	00:00:27	00:00:21	00:00:18	00:00:16
SS100	00:00:52	00:00:34	00:00:24	00:00:20	00:00:17	00:00:16

Time value is in format hh:mm:ss